

Self-Assembly of Porphyrin Arrays via Coordination to Transition Metal Bisphosphine Complexes and the Unique Spectral Properties of the Product Metallacyclic Ensembles

Jun Fan,[†] Jeffery A. Whiteford,[†] Bogdan Olenyuk,[†] Michael D. Levin,[†] Peter J. Stang,^{*,†} and Everly B. Fleischer[‡]

Contribution from the Departments of Chemistry, University of Utah, Salt Lake City, Utah 84112, and University of California, Irvine, California 92697

Received November 17, 1998

Abstract: Self-assembly of predesigned angular and linear dipyrldiporphyrin modules with bisphosphine-coordinated Pd(II) and Pt(II) angular and linear modules leads to cyclic porphyrin arrays containing two or four units and ranging in size from 15 to 39 Å. Multinuclear NMR spectra indicate high symmetry for these macrocycles. Restriction in rotation of *trans*-DPyDPP groups around the axis defined by the terminal metal–nitrogen bonds distorts the symmetry of the tetramers, but the rotation is unrestricted at elevated temperatures. Chiral metal triflates containing *R*(+)- or *S*(-)-BINAP phosphines promote formation of enantiomeric macrocycles with a puckered geometry. CD spectra of the chiral macrocycles reveal a strong exciton coupling between the porphyrin chromophores in the tetramers. Emission spectra reveal moderate fluorescence quenching of the dipyrldiporphyrin fluorophores upon treatment with metal triflates and concomitant incorporation into the macrocycles.

Introduction

A significant amount of practical insight has been gained and correlated to natural chromophores by designing and comparing light harvesting porphyrin arrays and aggregates to monoporphyrin systems.¹ Various molecular devices based on oligoporphyrins have recently been engineered and prepared, such as artificial photosynthetic systems,² photoinduced picosecond molecular switches,³ optoelectronic gates,⁴ fluorescence quenching sensors,⁵ photonic wires,⁶ and cancer therapy agents.⁷ The porphyrin array architectures reported to date include linear chains,^{7,8} cyclic oligomers,⁹ squares,¹⁰ sheets and tapes,¹¹ stars,¹²

rosettes,¹³ dendrimers,¹⁴ and others.¹⁵ The porphyrin oligomers have been synthesized by either covalent attachment of the monomers^{3,4,7–9,10b,14} or methods of self-assembly.^{10a,c–13,15} Porphyrin arrays consisting of up to nine units have been reported.¹¹

Nevertheless, the challenge remains for the preparation of new porphyrin-containing oligomers with well-defined structure and properties, since the optimal molecular arrangement for various applications has yet to be realized. Moreover, we have found no reports of chiral porphyrin arrays with more than two units.¹⁶ Preparation of the porphyrin arrays in high yields and significant quantities is still problematic. One of the major obstacles for porphyrin derivatives is low solubility, which complicates scale-up and characterization of the products.¹ In

[†] University of Utah.

[‡] University of California, Irvine.

(1) For a comprehensive monograph, see: *The Porphyrins*; Dolphin, D., Ed.; Academic: New York, 1978.

(2) (a) Wasielewski, M. R. *Chem. Rev.* **1992**, *92*, 435. (b) Gust, D.; Moore, T. A.; Moore, A. L. *Acc. Chem. Res.* **1993**, *26*, 198. (c) Harriman, A.; Sauvage, J.-P. *Chem. Soc. Rev.* **1996**, *41*. (d) Van Patten, P. G.; Shreve, A. P.; Lindsey, J. S.; Donohoe, R. J. *J. Phys. Chem. B* **1998**, *102*, 4209.

(3) Gosztola, D.; Niemczyk, M. P.; Wasielewski, M. R. *J. Am. Chem. Soc.* **1998**, *120*, 5118.

(4) Wagner, R. W.; Lindsey, J. S.; Seth, J.; Palaniappan, V.; Bocian, D. F. *J. Am. Chem. Soc.* **1996**, *118*, 3996.

(5) De Silva, A. P.; Gunaratne, H. Q. N.; Gunnlaugsson, T.; Huxley, A. J. M.; McCoy, C. P.; Rademacher, J. T.; Rice, T. E. *Chem. Rev.* **1997**, *97*, 1515 and references therein.

(6) Wagner, R. W.; Lindsey, J. S. *J. Am. Chem. Soc.* **1994**, *116*, 9759.

(7) (a) Sousa, C.; Maziere, C.; Maziere, J. C. *Cancer Lett.* **1998**, *128*, 177. (b) deVree, W. J. A.; Essers, M. C.; Sluiter, W. *Cancer Res.* **1997**, *57*, 2555. (c) Jasat, A.; Dolphin, D. *Chem. Rev.* **1997**, *97*, 2267.

(8) (a) Taylor, P. N.; Wylie, A. P.; Huuskonen, J.; Anderson, H. L. *Angew. Chem., Int. Ed. Engl.* **1998**, *37*, 986. (b) Nishino, N.; Wagner, R. W.; Lindsey, J. S. *J. Org. Chem.* **1996**, *61*, 7534. (c) Wagner, R. W.; Johnson, T. E.; Lindsey, J. S. *J. Am. Chem. Soc.* **1996**, *118*, 11166. (d) Osuka, A.; Tanabe, N.; Zhang, R. P.; Maruyama, K. *Chem. Lett.* **1993**, *9*, 1505. (e) Hammel, D.; Erk, P.; Schuler, B.; Heinze, J.; Müllen, K. *Adv. Mater.* **1992**, *4*, 737.

(9) (a) Vidal-Ferran, A.; Clyde-Watson, Z.; Bampos, N.; Sanders, J. K. M. *J. Org. Chem.* **1997**, *62*, 240. (b) Anderson, S.; Anderson, H. L.; Sanders, J. K. M. *J. Chem. Soc., Perkin Trans. 1* **1995**, 2255.

(10) (a) Drain, C. M.; Lehn, J. M. *J. Chem. Soc., Chem. Commun.* **1994**, 2313. (b) Wagner, R. W.; Seth, J.; Yang, S. L.; Kim, D.; Bocian, D. F.; Holten, D.; Lindsey, J. S. *J. Org. Chem.* **1998**, *63*, 5042. (c) Slone, R. V.; Hupp, J. T. *Inorg. Chem.* **1997**, *36*, 5422.

(11) Drain, C. M.; Nifiatis, F.; Vasenko, A.; Bateas, J. D. *Angew. Chem., Int. Ed. Engl.* **1998**, *37*, 2344.

(12) Yuan, H.; Thomas, L.; Woo, L. K. *Inorg. Chem.* **1996**, *35*, 2808.

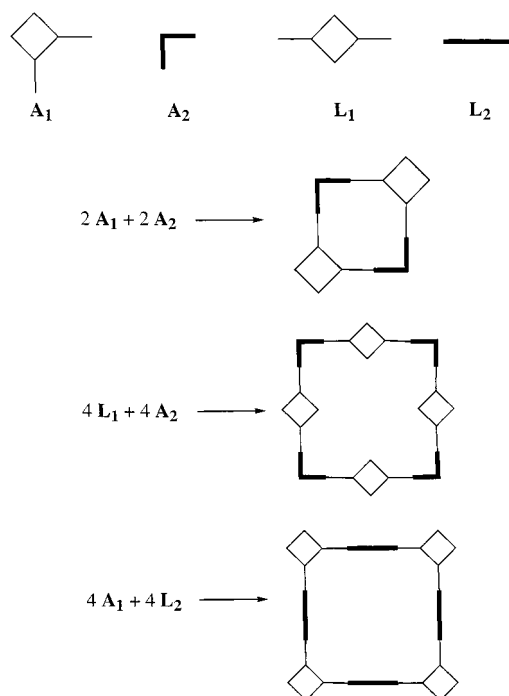
(13) Drain, C. M.; Russell, K. C.; Lehn, J.-M. *Chem. Commun.* **1996**, 337.

(14) Xu, Z.; Moore, J. S. *Acta Polym.* **1994**, *45*, 83.

(15) (a) Alessio, E.; Macchi, M.; Heath, S.; Marzilli, L. G. *Inorg. Chem.* **1997**, *36*, 5614. (b) Alessio, E.; Macchi, M.; Heath, S.; Marzilli, L. G. *J. Chem. Soc., Chem. Commun.* **1996**, 1411. (c) Kobuke, Y.; Miyaji, H. *Bull. Chem. Soc. Jpn.* **1996**, *69*, 3563. (d) Stibrany, R. T.; Vasudevan, J.; Knapp, S.; Potenza, J. A.; Emge, T.; Schugar, H. J. *J. Am. Chem. Soc.* **1996**, *118*, 3980. (e) Tamiaki, H.; Miyatake, T.; Tanikaga, R.; Holzwarth, A. R.; Schaffner, K. *Angew. Chem., Int. Ed. Engl.* **1996**, *35*, 772. (f) Amabilino, D. B.; Dietrich-Buchecker, C. O.; Sauvage, J.-P. *J. Am. Chem. Soc.* **1996**, *118*, 3285. (g) Rao, T. A.; Maiya, B. G. *J. Chem. Soc., Chem. Commun.* **1995**, 939. (h) Anderson, S.; Anderson, H. L.; Sanders, J. K. M. *Acc. Chem. Res.* **1993**, *26*, 469.

(16) For examples of chiral self-assembled macrocycles see: (a) Müller, C.; Whiteford, J. A.; Stang, P. J. *J. Am. Chem. Soc.* **1998**, *120*, 9827. (b) Stang, P. J.; Olenyuk, B. *Angew. Chem., Int. Ed. Engl.* **1996**, *35*, 732. (c) Olenyuk, B.; Whiteford, J. A.; Stang, P. J. *J. Am. Chem. Soc.* **1996**, *118*, 8221.

Scheme 1



this paper, we describe the preparation of well-defined, highly soluble, readily available, macrocyclic arrays of two or four pyridyl-substituted porphyrins by self-assembly with bisphosphine-coordinated transition metal triflates.¹⁷ We have synthesized achiral and chiral cyclic arrays and studied their structure and properties by NMR, UV, emission, and CD spectroscopic techniques.

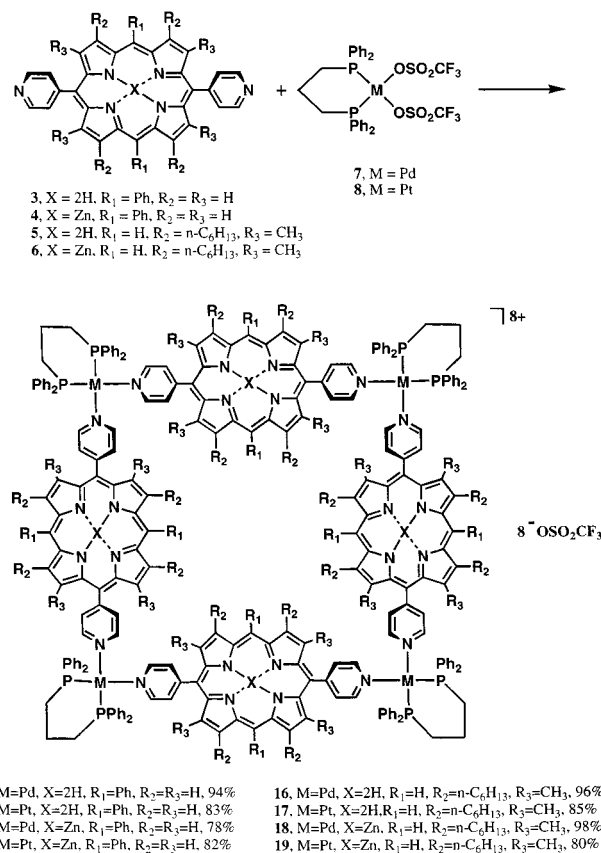
Results and Discussion

Design of Macrocycles. The self-assembly of rigid macrocycles requires well-defined, geometrically templated, building block precursors.¹⁸ Specifically, the assembly of square-shaped arrays requires four preprogrammed, 90° angular modules, which may be supplemented by four linear modules. Di(4'-pyridyl)porphyrins substituted in positions 5 and 10 or 5 and 15 (**1–6**) can serve as the angular or linear building blocks, respectively. Square-shaped arrays of three types have been prepared based on the di(4'-pyridyl)porphyrins (Scheme 1). In the smaller macrocycles two 5,10-di(4'-pyridyl)porphyrins (**1**, **2**, modules A_1) alternate with two transition metal-based angular units A_2 (**7–10**). 5,15-Di(4'-pyridyl)porphyrins (**3–6**) are used as the linear modules L_1 spanning four angular units A_2 . Finally, four porphyrin-containing angular blocks A_1 have been used to connect four platinum-terminated linear modules L_2 . Both free base porphyrin (**1**, **3**, and **5**) and zinc porphyrin derivatives (**2**, **4**, and **6**) are employed as the modules A_1 and L_1 . Bistriflates of 1,3-bis(diphenylphosphino)propane (dppp), 2,2'-bis(diphenylphosphino)-1,1'-binaphthyl (BINAP), dpppPd(II) (**7**), dpppPt(II) (**8**), and $R(+)$ -, $S(-)$ -BINAP-Pd(II) (**9** and **10**) have been used as precursors for the angular units A_2 , and 1,4-bis-[*trans*-Pt-(PEt₃)₂(OTf)]benzene (**11**) has been used as the precursor for the linear units L_2 . The geometrical parameters of the molecular

Table 1. Size of Various Porphyrin Tetramers Based on MM2 Calculations

building modules		corresponding macrocycles	diagonal (Å)	side (Å)
linear	angular			
none	$2A_1 + 2A_2$	20–23 , 29 , 30	15	12
$4L_1$	$4A_2$	12–19 , 26–28	29	20
$4L_2$	$4A_1$	24 , 25	39	24

Scheme 2



squares, as evaluated by molecular modeling (modified MM2),¹⁹ are listed in Table 1.

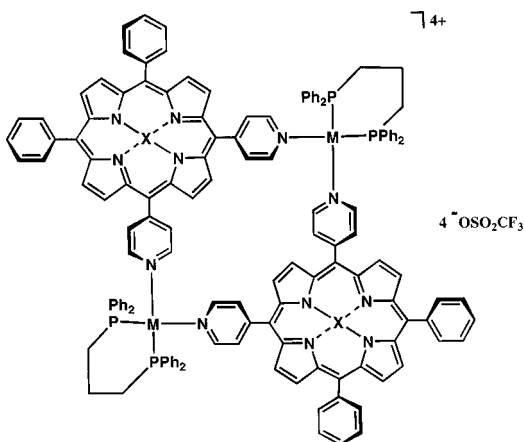
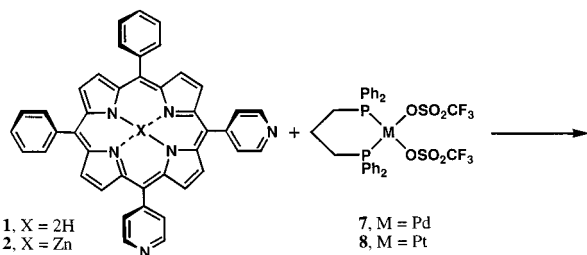
Synthesis and General Properties of Macrocycles. Achiral cyclic tetramers **12–19** were obtained by reacting bistriflates of dpppPd(II) or dpppPt(II) (**7** and **8**) with 5,15-di(4'-pyridyl)-10,20-diphenylporphyrin (*trans*-DPyDPP) (**3**), 5,15-di(4'-pyridyl)-3,7,13,17-tetramethyl-2,8,12,18-tetrahexylporphyrin (*trans*-DPyTTP) (**5**), and their zinc-containing analogues **4** and **6** (Scheme 2). The triflates **7** and **8** were also reacted with 5,10-di(4'-pyridyl)-15,20-diphenylporphyrin (*cis*-DPyDPP) (**1**) and *cis*-ZnDPyDPP (**2**) to yield the smaller macrocycles **20–23** (Scheme 3). Larger macrocycles **24** and **25** resulted from the reaction between the angular porphyrin precursors **1** and **2** and 1,4-bis[*trans*-Pt(PEt₃)₂(OTf)]benzene (**11**, Scheme 4). The chiral macrocycles **26** and **27** were formed in good yields by the reaction of *trans*-DPyDPP (**3**) with pure R (+)- or S (-)-BINAP-Pd(II) bistriflates **9** and **10** (Scheme 5). *trans*-ZnDPyDPP (**4**) yielded the tetramer **28** upon reaction with **9**. Reaction of *cis*-DPyDPP (**1**) with the triflates **9** and **10** gave access to the chiral dimer macrocycles **29** and **30**, respectively (Scheme 6).

(17) For a preliminary communication see: Stang, P. J.; Fan, J.; Olenyuk, B. *J. Chem. Soc., Chem. Commun.* **1997**, 1453.

(18) (a) Olenyuk, B.; Fechtenkötter, A.; Stang, P. J. *J. Chem. Soc., Dalton Trans.* **1998**, 1707. (b) Stang, P. J.; Olenyuk, B. *Acc. Chem. Res.* **1997**, *30*, 502 and references therein. (c) Fujita, M. *J. Synth. Org. Chem., Jpn.* **1996**, *54*, 953 and references therein.

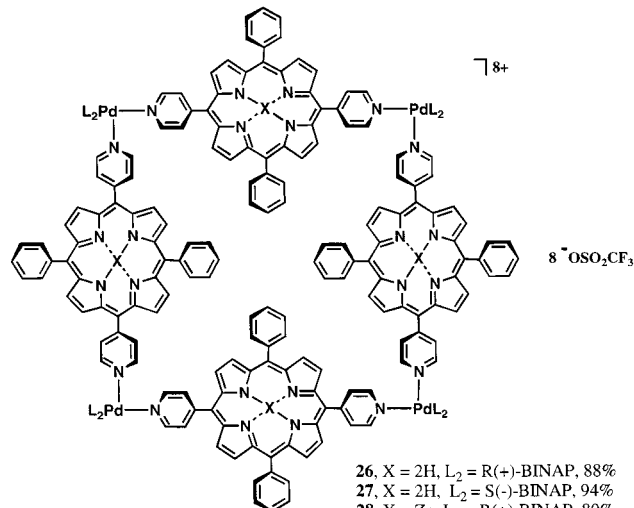
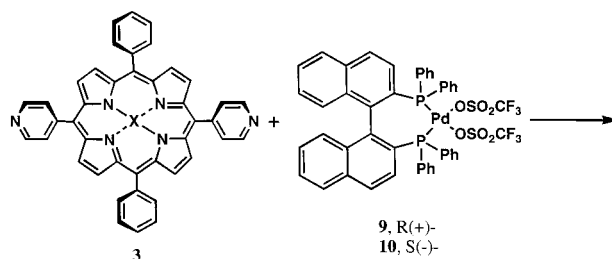
(19) (a) MM2 single point calculations and geometry optimization was performed with CS Chem3D Pro, Version 3.5.1, CambridgeSoft Corporation, 875 Massachusetts Avenue, Cambridge, MA 02139. (b) ESFF potential set geometry optimization was performed with INSIGHT II (97.0) and Discover 3, BIOSYM. The dielectric constant was set to 8.0.

Scheme 3



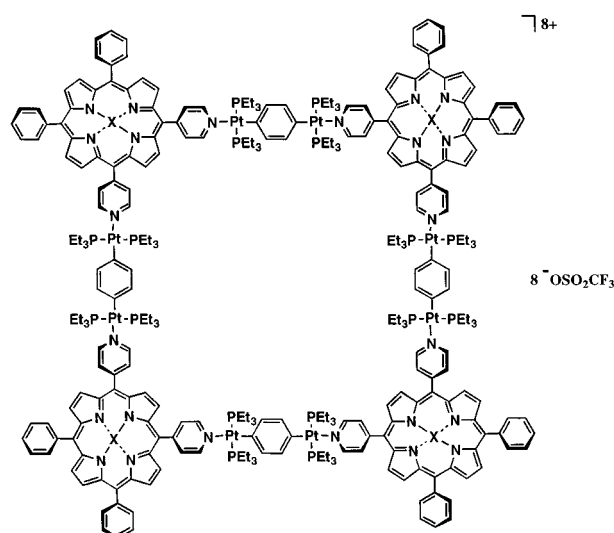
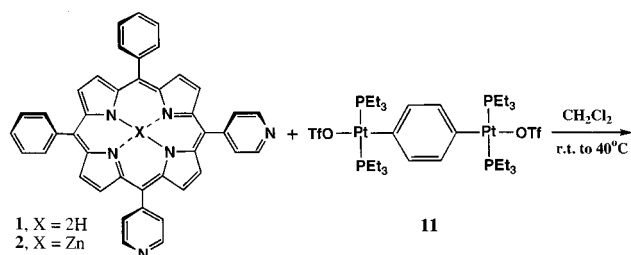
20, M = Pd, X = 2H, 93%
21, M = Pt, X = 2H, 80%
22, M = Pd, X = Zn, 93%
23, M = Pt, X = Zn, 82%

Scheme 5



26, X = 2H, L₂ = R(+)-BINAP, 88%
27, X = 2H, L₂ = S(-)-BINAP, 94%
28, X = Zn, L₂ = R(+)-BINAP, 80%

Scheme 4



24, X = 2H, 95%
25, X = Zn, 85%

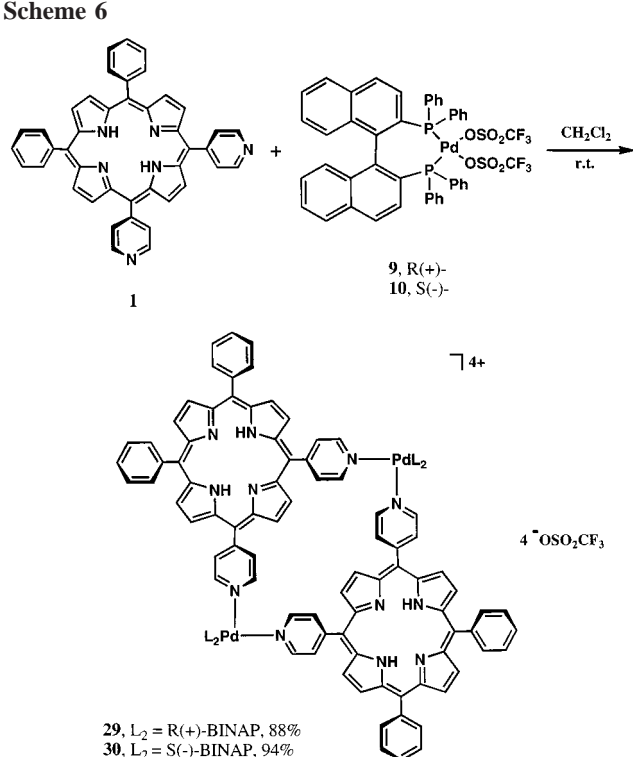
Since both reagents in these reactions contain variable amounts of water, it is necessary to monitor the stoichiometry of the reagents by NMR while preparing these assemblies. The pyridyl-containing reagent has a characteristic signal for the

α -pyridyl protons in the ¹H NMR spectra, while the metal-containing reagent has a distinctive signal for the bisphosphine ligands in the proton-decoupled ³¹P NMR spectra. Excess of either reagent can be quenched with the other reagent without significant effect on the yield. When the correct stoichiometry is achieved, the corresponding signals of the starting materials disappear. The formation of the respective macrocycle is complete when the line width of the ³¹P{¹H} NMR signal reaches its minimum.

Dichloromethane is the preferred solvent in most cases, but acetone or mixtures of chloroform and methanol are required for the zinc-containing porphyrins 2, 4, and 6 because of low solubility in dichloromethane. Longer reaction times and higher temperatures are usually needed for the completion of the reactions involving zinc-containing porphyrin derivatives, and somewhat lower isolated yields are observed in these reactions. Formation of the dimer macrocycles 20–23 proceeds faster than that of the tetramer macrocycles. The purple-red microcrystalline macrocycles precipitate out of the reaction mixture upon addition of diethyl ether. Analytically pure samples are obtained by redissolving the assemblies in the original solvent and recrystallizing them upon slow infusion of diethyl ether.

Interestingly, all macrocycles are more soluble than the precursor porphyrins alone. Presumably, the positive charge of the macrocycles and the arrangement of the phosphine ligands is such that they project out of the plane defined by the corners of the macrocycles, and prevent intermolecular stacking. This makes the crystal packing less thermodynamically favorable, and, thus, increases the solubility of the macrocycles. In this respect, the bisphosphine-coordinated Pd(II) and Pt(II) angular modules have solubility advantages over the analogous neutral transition metal chlorides used previously.^{10a,11} The higher solubility of the charged porphyrin oligomers allows one to carry out self-assembly on a preparative scale at a higher concentration without precipitation of the intermediates.

Scheme 6



The tetramers are stable below 240 °C, while the dimers decompose when heated above 350 °C. The decomposition temperature of the Pt-based macrocycles is 30–40 °C higher than those of their Pd-based analogues. Additionally, the macrocycles are somewhat hydroscopic in the solid state and light sensitive in solution.

NMR Spectra

trans-Dipyridylporphyrin Tetramers. The macrocycles **12**–**15** have complex, but similar ¹H NMR spectra. The assignment of the aromatic region of the ¹H NMR spectrum of **13** in acetone-*d*₆ (Figure 1) was based on a ¹H–¹H COSY NMR spectrum and by comparison with the spectra of other dppp chelated macrocycles. The doublets at δ 9.7 and 8.4 ppm are due to the α- and β-protons of the pyridyl moieties. The signals of the α-protons in **12**–**15** are significantly shifted downfield compared to those in the parent porphyrin due to coordination of the pyridyl group to a metal.^{10a,c,12} The four signals between δ 8.1 and 9.1 ppm are attributed to the porphyrin-bound protons (H_p and H_{p'}). The number of these signals is twice as large as the number of the corresponding signals in the parent *trans*-DPyDPP (**3**). The doubling of the number of signals is caused by the orientation of the porphyrin rings in the macrocycle such that half of the protons (H_{p'}) are located inside of the macrocycle, while the other half (H_p) are located outside of the macrocycle. The intense signals at δ 8.3 and 7.8 ppm are assigned to the phenyl-bound protons of the dppp groups (H_L). Finally, the four signals at δ 8.3,²⁰ 8.0, 7.0, and 6.1 ppm are due to the protons attached to the phenyl groups in positions 10 and 20 on the porphyrin rings (H_{ph} and H_{ph'}). As in the case of the signals of the porphyrin-bound protons, the large number of signals from the phenyl-bound H_{ph} and H_{ph'} is due to inequivalent phenyl groups located inside and outside of the macrocycle, respectively.

(20) This signal overlaps in the 1D ¹H NMR spectrum with a signal of dppp phenyl-bound protons. It has been assigned based on the ¹H–¹H COSY NMR spectrum of **13**.

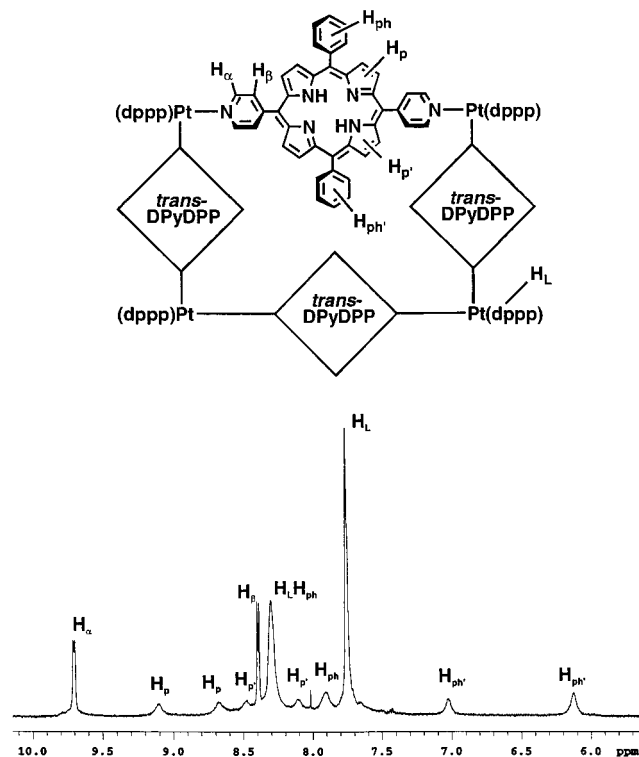


Figure 1. Assignment of the aromatic region of the ¹H NMR spectrum of tetramer **13**, 5.5 × 10⁻³ M in acetone-*d*₆ at ambient temperature.

These spectroscopic data are in accord with the results of molecular modeling of the structure of tetramers **12**–**15** and with studies of restricted rotation in pyridine–transition metal complexes.²¹ At the optimized geometries (modified MM2)¹⁹ for the tetramers, the pyridyl groups are perpendicular to the coordination plane of the metals and the plane of the porphyrin rings. This forces the porphyrin rings to be nearly coplanar with each other resulting in a planar macrocycle. Rotation around the metal–nitrogen bonds and the bonds between the pyridyl and porphyrin moieties is slow at ambient temperature on the NMR time scale, and this causes splitting of the signals and/or broadening of the lines in the spectra.^{16c} The line widths and the splitting patterns vary with solvent, temperature, and the coordinated metal. In less polar solvents (e.g. chloroform as compared to acetone) the signals due to the pyridyl-bound α-protons and the phenyl-bound dppp protons are broader, and the splitting between the signals of the porphyrin-bound protons is larger. This splitting is reduced at elevated temperatures. In the dpppPd-based tetramer **12**, the upfield signals, attributed to the phenyl-bound protons of the *trans*-DPyDPP moiety (H_{ph} and H_{ph'}), coalesce around 60 °C in CDCl₃ solution. For the dpppPt-based tetramer **13** the effect of temperature is less pronounced, and the coalescence cannot be reached below the boiling point of CDCl₃ at ambient pressure. Restriction in rotation around the metal–nitrogen bonds is relaxed at elevated temperature and in more polar solvents. The fact that the ligands rotate faster in the Pd-based macrocycles compared to the Pt-based analogues is in accord with the previous studies of such rotation.²¹

The ³¹P{¹H} NMR spectra of each of the tetramers **12** and **14** consist of one singlet at ambient conditions. The ³¹P{¹H} NMR spectra of tetramers **13** and **15** are similar to those of **12** and **14**, except that they contain platinum satellites due to the ¹⁹⁵Pt–³¹P spin–spin coupling. Compared to the ³¹P{¹H} NMR

(21) (a) Fuss, M.; Siehl, H.-U.; Olenyuk, B.; Stang, P. *Organometallics* **1999**, *18*, in press. (b) Stang, P. J.; Olenyuk, B.; Arif, A. M. *Organometallics* **1995**, *14*, 5281.

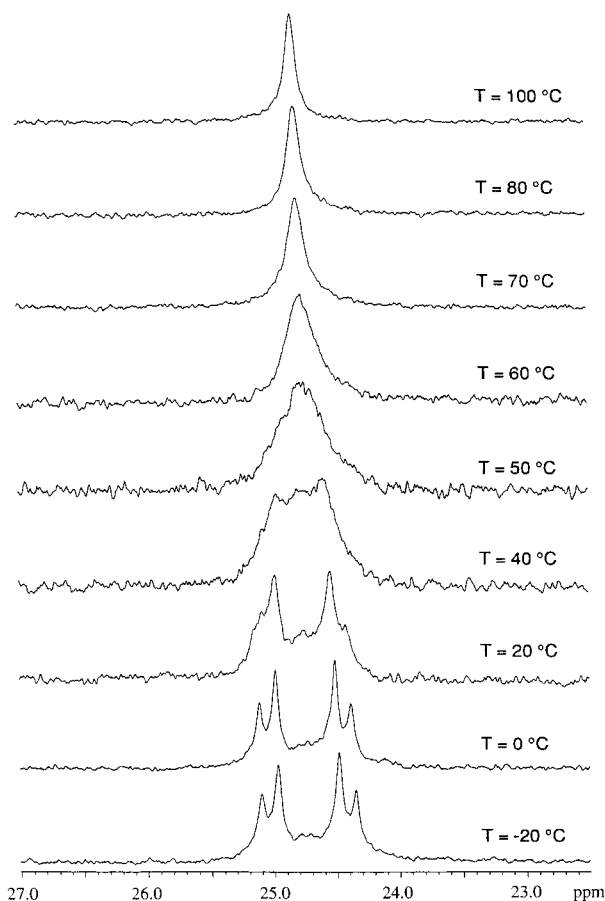


Figure 2. $^{31}\text{P}\{^1\text{H}\}$ NMR spectra of the tetramer **26** in a CD_3NO_2 solution at various temperatures.

signals of the bistriflates **7** and **8**, the tetramer signals are shifted upfield by ~ 10 ppm, indicative of the coordination of the nitrogen lone pair to the transition metal.²² The singlet in the spectrum of **13** splits into two below 0°C in CDCl_3 . The splitting of the signal is most likely due to the slow interconversion of conformers with inequivalent phosphorus nuclei. The conformers may be formed in two ways. If all four metal corners are in one plane, the conformers will differ by the mutual orientation of the porphyrin moieties with their parts inside and outside of the macrocycle above or below the plane. If the geometry of the cyclic tetramers is puckered, the conformers will differ by the relative arrangement of the porphyrin cores to the puckering angle. In the former case, the coalescence of the $^{31}\text{P}\{^1\text{H}\}$ NMR signals in the tetramers corresponds to the unfreezing of the restricted rotation of the porphyrin modules so that they can turn around the coplanar arrangement, but still cannot rotate freely around the axis defined by the metals. In the latter case, coalescence of the signal suggests unfreezing of the puckering motion in the macrocycles.

The $^{31}\text{P}\{^1\text{H}\}$ NMR spectra of the chiral phosphine containing tetramers **26**, **27**, and **28** consist of two signals. The major signal has an AB pattern, caused by the spin–spin coupling of two inequivalent ^{31}P nuclei coordinated to the same metal. A less intense broad signal appears close to the center of the AB pattern of the major signal. In the case of the macrocycle **26**, these two signals collapse into one sharp singlet at ca. 60°C in a CD_3NO_2 solution (Figure 2). The changes are reversible upon cooling. This observation allows the assignment of the AB pattern to the most favorable macrocycle conformer, while the minor

signals are presumably due to one or more other conformers. Analysis of the possible mutual arrangements of the porphyrin modules in the tetramers (Figure 3) shows that only two conformers possess the required symmetry to give the experimentally observed $^{31}\text{P}\{^1\text{H}\}$ NMR spectrum. A dome-shaped structure **I**, where the four transition metals define the plane, is in the C_4 symmetry point group (Figure 3a) while the puckered configuration **II** is defined as D_2 (Figure 3b). In the latter structure the porphyrin rings are oriented such that two C_2 symmetry axes are passing through four *meso* carbon atoms of the opposite side rings. Each structure contains four equivalent biphosphine ligands, with a pair of inequivalent phosphorus nuclei at each metal center. Molecular modeling (modified MM2 and ESFF)¹⁹ suggests that structure **II** has a lower energy than structure **I**. Furthermore, no local minimum has been found for a structure with C_4 symmetry. Geometry optimization (ESFF) yielded several local minima (e.g., **III**, Figure 3c) with structures similar to **II**. All these structures have the same puckered geometry but differ in the relative orientation of the porphyrin rings, which are con- or disrotated by about 30° around the Pd–Pd axis. This relieves some strain from steric interaction between the porphyrin-bound phenyl groups. Apparently, structure **II** is the average of the less symmetric structures with local minima, which is in agreement with the ^{31}P NMR data. Furthermore, the puckered structure is also favored by the BINAP-coordinated metal corners since they prefer the pyridyl ligand planes with a dihedral angle less than 90° .

Interestingly, the coalescence of the signals in the ^{31}P NMR spectra of the BINAP-containing tetramer **26** occurs at a much higher temperature than that of the analogous dppp-containing tetramer **13**. Assuming the puckered structure **II** for the tetramer **26**, the difference in the coalescence temperatures can be explained by a difference in the mechanism by which the macrocycles **13** and **26** increase their symmetry, or by a different barrier to puckering in the corresponding macrocycles.

cis-Dipyridylporphyrin Dimers and Tetramers. The spectra of the *cis*-DPyDPP dimers **20–23** and tetramers **24** and **25** are similar to those of the *trans*-DPyDPP tetramers **12–15**. The signals in the ^1H NMR spectra of the dimers **20–23** are narrower compared to those of **12–15**, presumably due to the lack of conformational changes at ambient temperature on the NMR time scale. The ^1H NMR spectra of the tetramers **24** and **25** are simpler than those of the dppp-containing macrocycles since they do not contain the signals from the dppp phenyl groups. The signals due to the pyridyl-bound protons in **24** and **25** are shifted upfield compared to those in the other macrocycles.

The $^{31}\text{P}\{^1\text{H}\}$ NMR spectra of the macrocycles **20–23** consist of single signals, which indicates that all the phosphorus nuclei are equivalent. The signals are shifted upfield by ca. 15 ppm compared to those of the starting bistriflates **7** and **8** as a result of a strong coordination of the pyridyl groups to the transition metals. The $^{31}\text{P}\{^1\text{H}\}$ NMR spectra of the macrocycles **24** and **25** consist of a singlet with two symmetrical satellites. The singlet is shifted upfield by 4 ppm compared to that of the starting bistriflate. The ^{19}F NMR spectrum of every individual macrocycle consists of one narrow singlet at around $\delta -77$ ppm, which is characteristic for an uncoordinated triflate anion.²³

Mass Spectrometry

Fast atom bombardment mass spectrometry (FABMS) analysis of **20** and **21** gave $M - \text{OTf}$ peaks of m/z 2716.5 and m/z 2895.8, respectively, with +1 charge states (i.e., separation of

(22) Stang, P. J.; Cao, D. H.; Saito, S.; Arif, A. M. *J. Am. Chem. Soc.* **1995**, *117*, 6273.

(23) Lawrance, G. A. *Chem. Rev.* **1986**, *86*, 17.

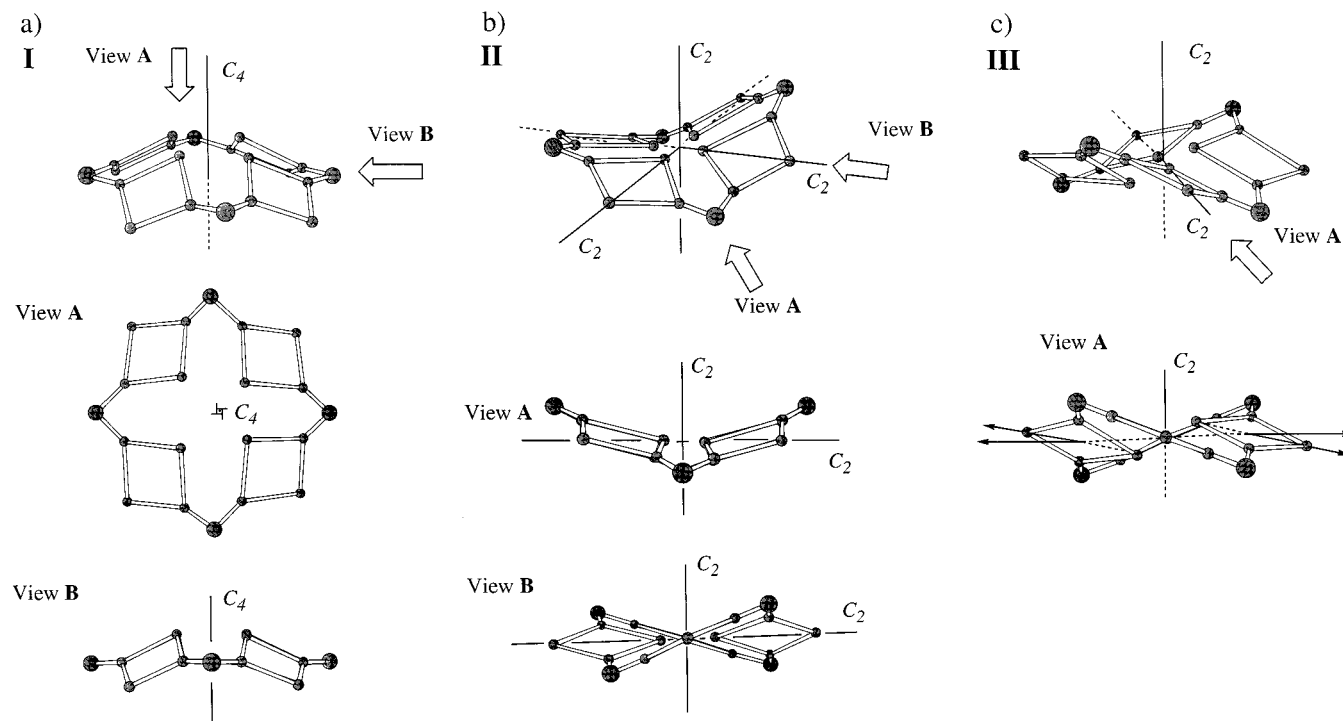


Figure 3. (a) Structure I: Only *meso*-carbons of porphyrins and Pd atoms are shown. (b) Structure II: Only *meso*-carbons of porphyrins and Pd atoms are shown. (c) Structure III: Only *meso*-carbons of porphyrins and Pd atoms are shown.

peaks by 1 m/z unit) resulting from a loss of one triflate from a total of four. Also indicative of the proposed molecule were the isotopic distribution patterns which were very close to the calculated compositions of the species. The calculated and experimental isotopic distribution patterns of the platinum analogue **21** are shown in Figure 4. Although this technique has been successful in producing evidence for the smaller macrocycles **20** and **21** and several other examples,²⁴ the upper molecular weight limit is approximately 4000–5000 amu. Alternatively, electrospray mass spectrometry (ESMS) has been successful in identifying the composition of larger aggregates and assemblies (5000–10000).²⁵ Application of this technique to macrocycle **16** gave similar results to previously reported examples studied by ESMS. The observation of the +4 species (1525.3 m/z) resulting from the loss of four triflate counterions (from a total of eight) and the isotopic distribution consistent with the theoretical isotopic envelope confirmed the composition of macrocycle **16**.

Absorption and Emission Spectra

The maxima of the Soret and Q-bands, characteristic for the porphyrin chromophores,²⁶ are red-shifted by 8–12 nm in the macrocycles **12–30** as compared to those of the starting porphyrins. This shift is more pronounced for the Pt-containing macrocycles. Analogous but smaller shifts have been reported for Pt(II)- and Pd(II)-coordinated monopyridyl porphyrin derivatives.¹²

The Soret bands of the macrocycles **12–30** are broader compared to those of the starting porphyrins **1–6**, which may be attributed to an intramolecular exciton coupling between the

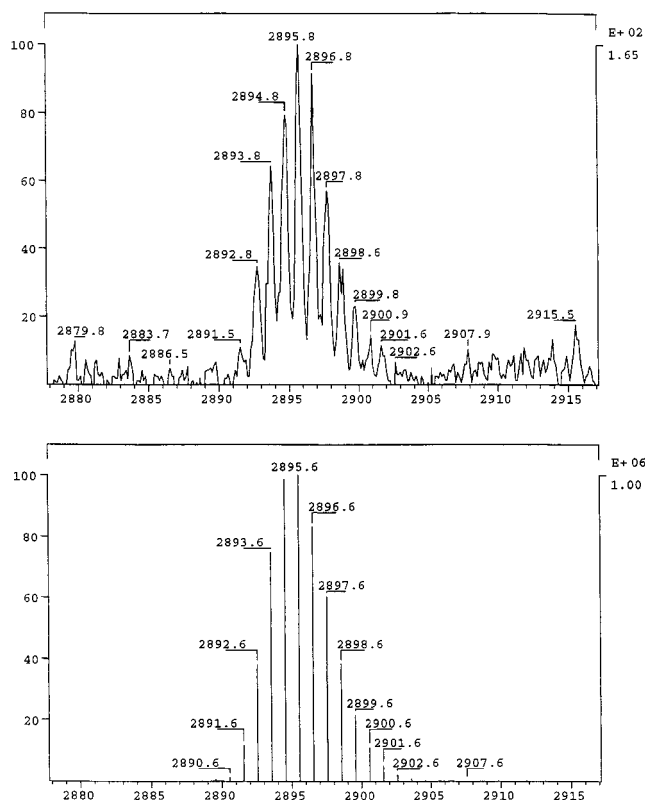


Figure 4. Experimental (top) and calculated (bottom) isotopic distribution pattern of $(M-OTf)^+$ for **21**.

porphyrin chromophores in the macrocycles. The extinction coefficient per porphyrin unit decreases upon formation of almost every macrocycle. The only exception is *trans*-ZnDPy-DPP (**4**). Its absorption in solution is depressed (ϵ 79 000 $\text{mol}^{-1} \times \text{cm}^{-1}$ at λ 420 nm) compared to other similar porphyrins (ϵ ca. 350 000 $\text{mol}^{-1} \times \text{cm}^{-1}$), presumably due to an extensive intermolecular coordination of the pyridyl groups to the zinc

(24) Whiteford, J. A.; Rachlin, E. M.; Stang, P. J. *Angew. Chem., Int. Ed. Engl.* **1996**, *35*, 2524. mass spec ref 4000–5000 mw limit.

(25) Manna, J.; Kuehl, C. J.; Whiteford, J. A.; Stang, P. J.; Muddiman, D. C.; Hofstadler, S. A.; Smith, R. D. *J. Am. Chem. Soc.* **1997**, *119*, 11611. mass spec ref 5000–10000 mw limit.

(26) Gouterman, M. In *The Porphyrins*, Vol. 3, *Physical Chemistry*, Part A; Dolphin, D., Ed.; Academic: New York, 1978.

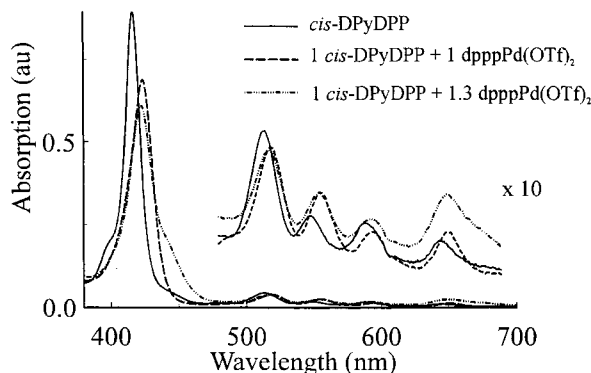


Figure 5. Absorption spectra of reaction mixtures of *cis*-DPyDPP (**1**) and *dppp*Pd(OTf)₂ (**7**), 5×10^{-6} M solution in CH₂Cl₂ at ambient temperature.

atoms.²⁷ The molar absorptions of the *trans*-ZnDPyDPP-containing macrocycles **13** and **15**, however, are comparable to those of the similar macrocycles **12**, **14**, and **16–30**. Thus, we observe a significant increase in the extinction coefficient per porphyrin unit upon incorporation of *trans*-ZnDPyDPP in the macrocycles **13** and **15**.

An interesting observation is that the porphyrins incorporated in the macrocycles do not possess a shoulder to their Soret band due to the B(0–1) transition.²⁶ The only exceptions are the macrocycles **26** and **27** with the BINAP–Pd(II) corners. If an excess of the metal-containing reagent is present in the reaction mixture, a distinct shoulder to the Soret band of a porphyrin at longer wavelengths (usually ca. 460 nm) is observed (Figure 5).

A steady decrease in fluorescence is observed upon titration of *trans*-DPyDPP or *cis*-DPyDPP solutions with solutions of *dppp*–metal triflates in CH₂Cl₂. An overall 30–60% drop in fluorescence of the porphyrins is observed upon formation of the macrocycles. The fluorescence of the macrocycles is suppressed even further upon addition of excess of the *dppp*–metal triflates. The decrease in fluorescence is more pronounced upon addition of *dppp*Pt(II) than *dppp*Pd(II) triflate. This observation is in accord with an assumption that the heavy-atom effect is the major contributor to the fluorescence quenching.²⁸

CD Spectra of Macrocycles Containing Chiral Bisphosphines

A striking feature of the CD spectra of the tetramers **26** and **27** is the bisignate curve (positive and negative components) between 400 and 450 nm (Figure 6). It is probably due to exciton coupling between two or more porphyrin chromophores of the macrocycle.²⁹ The apparent Davydov splitting^{29,30} is 10 nm. The amplitude of the splitting is quite impressive: $\Delta\epsilon = 1800 \text{ L} \times \text{mol}^{-1} \times \text{cm}^{-1}$. This amplitude is inversely proportional to the square of the interchromophore distance³¹ and proportional to the square of the extinction coefficients.³² An extremely high

(27) (a) Hunter, C. A.; Hyde, R. K. *Angew. Chem., Int. Ed. Engl.* **1996**, *35*, 1936. (b) Fleischer, E. B.; Shachter, A. M. *Inorg. Chem.* **1991**, *30*, 3763.

(28) Klessinger, M.; Michl, J. *Excited States and Photochemistry of Organic Molecules*; VCH: New York, 1995.

(29) Harada, N.; Nakanishi, K. *Circular Dichroic Spectroscopy*; University Science Books: Mill Valley, CA, 1983.

(30) (a) Harada, N.; Nakanishi, K. *Acc. Chem. Res.* **1972**, *5*, 257. (b) Davydov, A. S. *Theory of Molecular Excitons*; McGraw-Hill: New York, 1962.

(31) Harada, N.; Chen, S.-M.; Nakanishi, K. *J. Am. Chem. Soc.* **1975**, *97*, 5345.

(32) Heyn, M. P. *J. Phys. Chem.* **1975**, *79*, 2424.

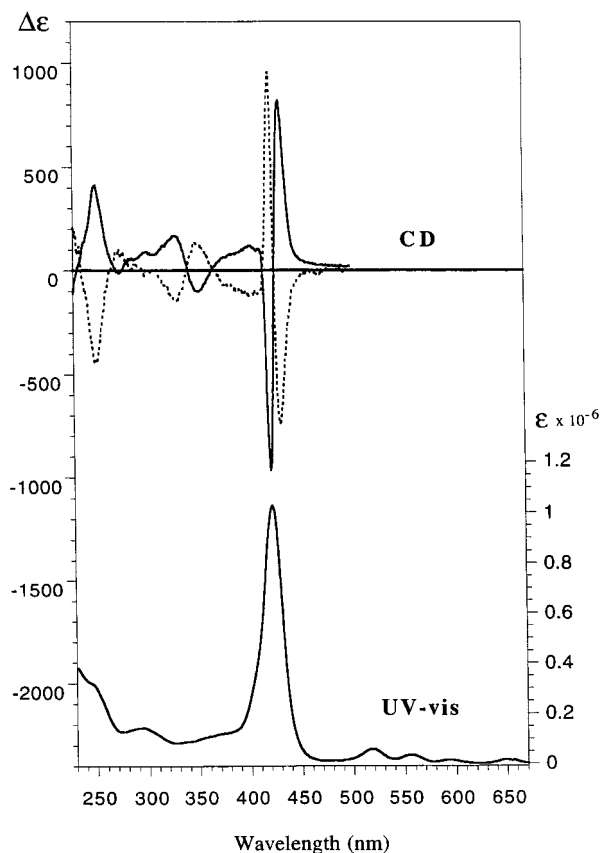


Figure 6. CD and UV-vis spectra of the tetramer **26** (solid line) and **27** (dashed line), 1.1×10^{-6} M solution in CH₂Cl₂ at ambient temperature.

extinction coefficient of the porphyrin chromophores provides for a very strong exciton coupling in the macrocycles.³³ However, even taking into account the short interchromophore distances of ca. 14 Å between the adjacent porphyrin cores and ca. 21 Å between the porphyrin cores opposite one another, the observed magnitude of the splitting may be explained only by a cooperative interaction between several porphyrin chromophores.

Three types of coupling interactions may exist between the four porphyrin chromophores in **26** and **27**: (a) four “adjacent” porphyrin couplings (pairs of porphyrins attached to the same transition metal corner), (b) two “opposing” porphyrin couplings (porphyrins on opposing sides of the macrocycle), and (c) a combination of a and b. Examination of structure **II** reveals that both the “adjacent” and the “opposing” pairs of porphyrin chromophores are in the same chiral environment of the BINAP ligands. This is in accord with the signs of the first and the second Cotton effects observed in the CD spectrum for the Soret band of the macrocycles **26** and **27**, as well as with the large magnitude of the splitting due to mutual cooperativity. The macrocycles **26** and **27** are enantiomers, hence their CD spectra are mirror images of each other.

No circular dichroism is observed for the Soret band of the zinc-containing tetramer **28** presumably because of the high symmetry (*D_{4h}*) of the zinc porphyrin chromophore.²⁶ Circular dichroism (ϵ 300 at λ 420 nm) without chiral exciton coupling is observed for the Soret band of the macrocycles **29** and **30**. This fact suggests that the two porphyrin cores are coplanar, and the consequent coplanarity of the transition moments of

(33) Matile, S.; Berova, N.; Nakanishi, K.; Fleischhauer, J.; Woody, R. *W. J. Am. Chem. Soc.* **1996**, *118*, 5198.

the chromophores prevents the coupling from being observed.²⁹ The dimers **29** and **30** are enantiomers and also give antipodal Cotton effects, respectively.

Conclusions

Macrocyclic assemblies, containing two or four porphyrin units, are readily obtained on a preparative scale via self-assembly with use of Pd(II)- or Pt(II)-containing auxiliary modules. The bisphosphine ligands coordinated to transition metals provide for an enhanced solubility of the macrocycles. The porphyrin cores are not coplanar when used as parts of the linear modules in the tetramers **12**–**19**. The barrier to rotation of the *trans*-DPyDPP moiety around the axis defined by the two metal–nitrogen bonds in the nonchiral tetramers depends on the type of transition metal used in the assembly and on the solvent. Two stages of unfreezing of the conformational motion are distinguished by NMR spectroscopy: initially the macrocycles adopt a coplanar arrangement, and at a high temperature the full rotation of the rings becomes fast on the NMR time scale. Chiral macrocycles are formed upon employment of the BINAP–Pd(II) angular building block. The chiral tetramers have a puckered structure of *D*₂ symmetry at ambient temperature. The porphyrin chromophores in the enantiomeric dimers **29** and **30** and the enantiomeric tetramers **26** and **27** show strong circular dichroism around 420 nm. Cooperative coupling of four excitons in the tetramers **26** and **27** leads to Davydov splitting with a very high amplitude. The high solubility and ease of synthesis of self-assembled porphyrin macrocycles, based on Pt(II) and Pd(II) phosphine bistriflates, provides tetramers that are excellent ensembles for the study of porphyrin exciton coupling interactions and induced circular dichroism (ICD).

Experimental Section

General Methods. All reactions were conducted under a dry nitrogen atmosphere following Schlenk techniques, although the products may be handled in air. IR spectra were recorded on a Mattson Polaris FT-IR spectrometer. UV–vis spectra were obtained with use of a Hewlett-Packard 8452A UV–vis spectrophotometer. Circular dichroism (CD) spectra were recorded on an Aviv 62ADS CD spectrometer. Optical rotations were measured on a Perkin-Elmer 241MC polarimeter. NMR spectra were recorded on a Varian Unity-300, Varian XL-300, or Varian VXR-500 spectrometer. The ¹H NMR spectra were recorded at 300 or 500 MHz, and chemical shifts are reported relative to internal TMS δ 0.0 ppm or to the signal of a residual protonated solvent: CDHCl₂ δ 5.32 ppm, CHCl₃ δ 7.27 ppm, or (CD₃)CO(CD₂H) δ 2.05 ppm. The ¹³C{¹H} NMR spectra were recorded at 75 or 125 MHz, and chemical shifts are reported relative to CD₂Cl₂ δ 54.00 ppm or CDCl₃ δ 77.23 ppm. The ¹⁹F NMR spectra were recorded at 282 MHz and chemical shifts are reported relative to external CFCl₃ δ 0.0 ppm. The ³¹P{¹H} NMR spectra were recorded at 121 or 202 MHz, and chemical shifts are reported relative to external 85% aqueous H₃PO₄ δ 0.0 ppm. The signals in ¹H NMR due to water are omitted. Elemental analyses were performed by Atlantic Microlab Inc., Norcross, GA. Melting points were obtained with a Mel-Temp capillary melting point apparatus and were not corrected. Mass spectra of **20** and **21** were obtained with a Finnigan MAT 95 mass spectrometer with a Finnigan MAT ICIS II operating system under positive fast atom bombardment (FAB) conditions at 20 keV. 3-Nitrobenzyl alcohol was used as a matrix in CHCl₃ as a solvent, and polypropylene glycol and cesium iodide were used as a reference for peak matching. Larger macrocycle (>5000 amu) **16** was analyzed with a Micromass Quatro II with ionization performed under electrospray conditions (flow rate 7.7 μL/min; capillary voltage 3.0 kV; cone 27 V; Extractor 12 V). About 15 individual scans were averaged for the mass spectrum. The calibration of the mass range 100–3000 amu was done with a 1:1 mixture of a 2-propanol–water solution of NaI (2 μg/μL) and CsI (0.01 μg/μL). Samples were prepared as 10 pg/μL solutions in acetone just prior to the analysis.

Materials. Commercial reagents were ACS reagent grade or higher and were used without further purification. Methylene chloride was purified according to literature procedure³⁴ and distilled over CaH₂. Diethyl ether was purified according to literature procedure³⁴ and distilled over Na/benzophenone. Methylene chloride and chloroform used for spectroscopic measurements were spectrophotometric grade. 3,3'-Dihexyl-4,4'-dimethyl-2,2'-dipyrrylmethane,³⁵ *cis*-DPyDPP (**1**),^{27b} *trans*-DPyDPP (**3**),^{27b} dpppPd(OTf)₂ (**7**),²² dpppPt(OTf)₂ (**8**),²² Pd(*R*)-BINAP(OTf)₂ (**9**),^{16c} Pd(*S*)-BINAP(OTf)₂ (**10**),^{16c} and 1,4-bis(*trans*-Pt(PEt₃)₂(OTf))benzene (**11**)²⁵ were prepared according to published procedures.

***cis*-ZnDPyDPP (**2**).** To a stirred solution of 100.0 mg (0.16 mmol) of **1** in a 70 mL of mixture of CHCl₃ and MeOH (3:1) was added 356 mg (1.6 mmol) of Zn(OAc)₂. The mixture was stirred and refluxed in the dark for 20 h. The solvent was removed in vacuo. The residue was washed with MeOH (3 × 20 mL). The product was dried in vacuo. Yield: 79 mg (73%). Mp > 400 °C dec. ¹H NMR (300 MHz, CDCl₃) δ 8.90 (s, 2H, H-17 and H-18), 8.76 (d, *J* = 3.9 Hz, 2H, H-2 and H-13), 8.15 (m, 6H, H-3, H-12, and Ph H_o), 7.98 (s, 2H, H-7 and H-8), 7.73 (m, 6H, Ph H_m, H_p), 7.17 (br, s, 4H, py H_β), 2.45 (s, 4H, py H_α). ¹³C{¹H} NMR (75 MHz, CDCl₃) δ 150.9 (s), 150.4 (s), 148.7 (s), 148.1 (s), 143.0 (s), 134.7 (s), 132.9 (s), 132.7 (s), 130.8 (s), 130.6 (s), 129.1 (m), 127.8 (s), 126.7 (s), 122.5 (s). UV–vis (CHCl₃) λ_{max} (ε) [nm (cm⁻¹ M⁻¹)] 422 (537 000), 552 (17 000), 600 (7000). MS (CI) *m/z* 679.2 (100, M⁺). Anal. Calcd for C₄₂H₂₆N₆Zn·H₂O: C, 72.26; H, 4.04; N, 12.04. Found: C, 71.79; H, 3.92; N, 11.85.

***trans*-ZnDPyDPP (**4**).** To a stirred solution of 30.0 mg (0.049 mmol) of **3** in a 40 mL mixture of CHCl₃ and MeOH (3:1) was added 106.6 mg (0.49 mmol) of Zn(OAc)₂. The mixture was stirred and refluxed in the dark for 10 h. The solvent was removed in vacuo. The residue was washed with MeOH (3 × 20 mL). The product was dried in vacuo. Yield: 34 mg (100%). Mp 360–362 °C dec. ¹H NMR (300 MHz, CDCl₃) δ 8.70 (d, *J* = 3.9 Hz), 8.08 (m), 7.70 (m), 7.20 (br, s, 4H, py H_β), 2.13 (s, 4H, py H_α). ¹³C{¹H} NMR (75 MHz, CDCl₃) δ 152.2 (s), 150.5 (s), 148.5 (s), 144.3 (m), 143.0 (s), 139.1 (s), 134.6 (s), 132.7 (s), 130.7 (s), 129.1 (s), 127.7 (s), 126.6 (s), 121.8 (s), 120.9 (s), 118.5 (s), 118.1 (s), 116.3 (m). UV–vis (CHCl₃) λ_{max} (ε) [nm (cm⁻¹ M⁻¹)] 418 (76 000), 548 (7000), 614 (4000).

***trans*-DPyTTP (**5**).** A solution of 380 mg (1.11 mmol) of 3,3'-dihexyl-4,4'-dimethyl-2,2'-dipyrrylmethane, 120 mg (1.11 mmol) of 4-pyridinecarboxaldehyde, and 56.8 mg (0.3 mmol) of *p*-toluenesulfonic acid in 14 mL of methanol was stirred for 6 h in the dark at ambient temperature and for 16 h at 0 °C. Then, 531 mg (2.34 mmol) of 2,3-dichloro-5,6-dicyano-1,4-benzoquinone (DDQ) was added and the mixture was stirred in the dark for an additional 4 h. The precipitate was filtered and washed with methanol. The filtrate was evaporated and the residue was treated with a 10% aqueous solution of NaOH, then with water. The black solid was dissolved in CH₂Cl₂ and filtered through a short pad of silica gel and further purified by column chromatography with a mixture of CH₂Cl₂ and ethyl acetate (3:1) as eluent. Yield: 50 mg (12%). Mp 250–252 °C dec. ¹H NMR (300 MHz, CD₂Cl₂, TMS) δ 10.28 (s, 2H, H-10 and H-20), 9.05 (d, *J* = 5.7 Hz, 4H, py H_α), 8.09 (d, *J* = 6.0 Hz, 4H, py H_β), 3.99 (t, *J* = 7.8 Hz, 8H, porph-CH₂-(CH₂)₄CH₃), 2.53 (s, 12H, porph-CH₃), 2.19 (m, 8H, porph-CH₂-CH₂-(CH₂)₂CH₃), 1.74 (m, 8H, porph-(CH₂)₂-CH₂-(CH₂)₂CH₃), 1.48 (m, 8H, porph-(CH₂)₃-CH₂-CH₂CH₃), 1.38 (m, 8H, porph-(CH₂)₄-CH₂CH₃), 0.91 (t, *J* = 7.2 Hz, 12H, porph-(CH₂)₅CH₃), -2.42 (s, 2H, NH). ¹³C{¹H} NMR (75 MHz, CD₂Cl₂, TMS) δ 150.8 (s, py C_γ), 149.2 (s, py C_α), 144.3 (s, porph C₄), 144.2 (s, porph C₁), 141.8 (s, porph C₃), 135.6 (s, porph C₂), 128.5 (s, py C_β), 114.8 (s, porph C₅-py), 97.7 (s, C₁₀), 33.6 (s, porph-CH₂), 32.2 (s, porph-CH₃), 30.2 (s, hexyl CH₂), 27.0 (s, hexyl CH₂), 23.0 (s, hexyl CH₂), 15.2 (s, hexyl CH₂), 14.4 (s, hexyl CH₃). IR (neat) 2930, 2854, 1590, 1462, 1286, 1129, 1068, 960, 759 cm⁻¹. UV–vis (CH₂Cl₂) λ_{max} (ε) [nm (cm⁻¹ M⁻¹)] 292 (493 000), 406 (180 400), 508 (186 000), 540 (87 000), 574 (87 000), 628 (36 000). MS (CI) *m/z* 857 (M⁺, 100).

***trans*-ZnDPyTTP (**6**).** To a stirred solution of 20.0 mg (0.023 mmol) of **5** in a 40 mL of mixture of CHCl₃ and MeOH (3:1) was added 51.2

(34) Perrin, D. D.; Armarego, W. L. F. *Purification of Laboratory Chemicals*; Pergamon Press: Oxford, 1988.

(35) Bao, Z.; Chen, Y.; Yu, L. *Macromolecules* **1994**, *27*, 4629.

mg (0.23 mmol) of Zn(OAc)₂. The mixture was stirred and refluxed in the dark for 3 h. The solvent was removed in vacuo. The residue was washed with MeOH (3 × 20 mL). The product was dried in vacuo. Yield: 17 mg (79%). Mp 284–286 °C dec. ¹H NMR (300 MHz, CDCl₃) δ 9.99 (s, 2H, H-10 and H-20), 3.81 (t, *J* = 5.0 Hz, 8H, porph-CH₂-(CH₂)₄CH₃), 2.04 (m, 8H, porph-CH₂CH₂-(CH₂)₃CH₃), 1.66 (br, s, 20H, porph-CH₃ and porph-(CH₂)₂CH₂-(CH₂)₂CH₃), 1.44 (m, 8H, porph-(CH₂)₃CH₂-CH₂CH₃), 1.34 (m, 8H, porph-(CH₂)₄CH₂-CH₃), 0.86 (t, *J* = 6.9 Hz, 12H, porph-(CH₂)₅CH₃). ¹³C{¹H} NMR (75 MHz, CDCl₃, TMS) δ 152.7 (s, py C_γ), 146.5 (s, py C_α), 146.1 (s, porph C₄), 143.9 (s, porph C₁), 136.4 (s, porph C₃), 136.3 (s, porph C₂), 127.8 (s, py C_β), 114.9 (s, porph C₅-py), 97.9 (s, C₁₀), 33.6 (s, porph-CH₂), 32.2 (s, porph-CH₃), 30.3 (s, hexyl CH₂), 27.0 (s, hexyl CH₂), 23.0 (s, hexyl CH₂), 15.3 (s, hexyl CH₂), 14.4 (s, hexyl CH₃). IR (neat) 2924, 1609, 1458, 1261, 1069 cm⁻¹. UV-vis (CH₂Cl₂) λ_{max} (ε) [nm (cm⁻¹ M⁻¹)] 412 (342 000), 540 (20 000), 576 (11 000). MS (CI) *m/z* 919 (M⁺, 100).

[Pd(dppp)(trans-DPyDPP)]₄[OTf]₈ (12). To a solution of 10.0 mg (0.012 mmol) of dpppPd(OTf)₂, **7**, in 5 mL of a 3:1 mixture of CHCl₃ and CH₃OH was added 7.5 mg (0.012 mmol) of porphyrin **3**, and the resulting solution was stirred at room temperature for 1 h. The solvent was reduced in volume to 1 mL in vacuo and ether was added resulting in the formation of a dark-red solid, which was collected, washed with ether, and dried in vacuo. Yield 16.4 mg (94%). Mp 304–306 °C dec. ¹H NMR (300 MHz, CDCl₃) δ 9.62 (s, 16H, py H_α), 8.93 (br, s, 8H, outer pyrrol H_β), 8.33 (m, 16H, pyrrol H_β), 8.12 (m, 36 H, py H_β, porph outer Ph H_{o,p}, pyrrol H_β), 7.68 (m, 32H, PhP H_o), 7.65 (m, 56H, porph outer Ph H_m, PhP H_{m,p}), 6.98 (br, s, 8H, porph inner Ph H_o), 6.04 (br, s, 12H, porph inner Ph H_{m,p}), 3.50 (m, 16H, PhP-CH₂), 2.56 (m, 8H, PhP-CH₂CH₂), -3.04 (s, 8H, NH). ¹³C{¹H} NMR (125 MHz, CDCl₃) δ 153.7 (s, py C_γ), 149.3 (s, py C_α), 143.3 (s), 141.1 (s), 134.8 (s, py C_β), 133.7 (m), 132.9 (s), 132.0 (s), 130.2 (s), 126.8 (s), 125.4 (m), 121.3 (q, *J* = 318 Hz, CF₃SO₃), 114.8 (s, porph C-5 and C-15), 95.0 (s, porph C-10 and C-20), 29.9 (PhP CH₂), 18.3 (s, PhPCH₂CH₂). ³¹P{¹H} NMR (121 MHz, CDCl₃, H₃PO₄) δ 3.9 (s). ¹⁹F NMR (282 MHz, CDCl₃, CFCl₃) δ -79.6 (s). UV-vis (CH₂Cl₂) λ_{max} (ε) [nm (cm⁻¹ M⁻¹)] 268 (151 000), 422 (918 000), 520 (77 000), 556 (52 000), 594 (29 000), 650 (35 000). Anal. Calcd for C₂₈₄H₂₁₆N₂₄P₈O₂₄S₈F₂₄Pd₄·8H₂O: C, 58.02; H, 3.98; N, 5.72; S, 4.36. Found: C, 57.72; H, 3.92; N, 5.63; S, 4.48.

[Pt(dppp)(trans-DPyDPP)]₄[OTf]₈ (13). A solution of 10.0 mg (0.011 mmol) of dpppPt(OTf)₂, **8**, in 5 mL of acetone was treated with 6.8 mg (0.011 mmol) of porphyrin **3** and the resulting solution was stirred at 40 °C for 4 h. The solvent was reduced in volume to 0.5 mL followed by addition of diethyl ether. The brown precipitate was collected, washed with ether, and dried in vacuo. Yield: 14.0 mg (83%). Mp 330–332 °C dec. ¹H NMR (500 MHz, acetone-*d*₆) δ 9.70 (d, *J* = 4.5 Hz, 16H, py H_α), 9.10 (s, 8H, outer pyrrol H_β), 8.68 (s, 8H, outer pyrrol H_β), 8.47 (s, 8H, inner pyrrol H_β), 8.39 (m, 24H, porph outer Ph H_o, py H_β), 8.30 (m, 32H, PhP H_o), 8.11 (s, 8H, inner pyrrol H_β), 7.90 (m, 12H, porph outer Ph H_{m,p}), 7.75 (m, 48H, PhP H_{m,p}), 7.03 (s, 8H, porph inner Ph H_o), 6.12 (s, 12H, porph inner Ph H_{m,p}), 3.78 (s, 16H, PhP-CH₂), 2.59 (m, 8H, PhP-CH₂CH₂), -3.03 (s, 8H, NH). ¹³C{¹H} NMR (125 MHz, CDCl₃) δ 154.3 (s, py C_γ), 149.4 (s, py C_α), 141.9 (s), 134.7 (m), 133.8 (m), 132.9 (s), 132.5 (s), 130.1 (s), 127.3 (m), 121.3 (q, *J* = 320 Hz, CF₃SO₃), 114.5 (s), 99.7 (s), 29.9 (PhP CH₂), 18.4 (s, PhPCH₂CH₂). ³¹P{¹H} NMR (202 MHz, acetone-*d*₆, H₃PO₄) δ -9.9 (*J*_{pt-p} = 3060 Hz). ¹⁹F NMR (282 MHz, CDCl₃, CFCl₃) δ -78.9 (s). UV-vis (CHCl₃) λ_{max} (ε) [nm (cm⁻¹ M⁻¹)] 426 (1 000 000), 518 (52 000), 558 (36 000), 592 (18 000), 652 (18 000). Anal. Calcd for C₂₈₄H₂₁₆N₂₄P₈O₂₄S₈F₂₄Pt₄·8H₂O: C, 54.72; H, 3.75; N, 5.39; S, 4.11. Found: C, 54.47; H, 3.67; N, 5.14; S, 3.91.

[Pd(dppp)(trans-ZnDPP)]₄[OTf]₈ (14). To a solution of 8.6 mg (0.013 mmol) of **4** in 5 mL of CHCl₃ was added 10.3 mg (0.013 mmol) of dpppPd(OTf)₂, **7**, and the solution was stirred at room temperature for 1 h. The solvent was reduced in volume to 0.5 mL in vacuo. Diethyl ether was then added and the dark-purple precipitate was filtered and dried in vacuo. Yield: 14.8 mg (78%). Mp 280–285 °C dec. ¹H NMR (300 MHz, CDCl₃/CD₃OD) δ 9.41 (br, s, 8H, outer pyrrol H_β), 9.33 (s, 16H, py H_α), 8.76–8.64 (m, 8H, outer pyrrol H_β), 8.25 (m, 16H, inner pyrrol H_β), 8.02–7.86 (m, 28H, porph outer Ph H_{o,p}, py H_β), 7.66–7.38 (m, 88H, porph outer Ph H_m, PhP H_{o,m,p}), 6.90

(br, s, 8H, porph inner Ph H_o), 5.95 (br, s, 12H, porph inner Ph H_{m,p}), 3.58 (s, 16H, PhP-CH₂), 2.43 (m, 8H, PhP-CH₂CH₂). ¹³C{¹H} NMR (125 MHz, CDCl₃/CD₃OD) δ 154.3 (s), 149.4 (s), 141.9 (s), 134.7 (m), 133.8 (m), 132.9 (s), 132.5 (s), 130.1 (s), 127.3 (m), 121.3 (q, *J* = 320 Hz, CF₃SO₃), 114.5 (s), 99.7 (s), 29.9 (s), 18.4 (s). ³¹P{¹H} NMR (121 MHz, CDCl₃/CD₃OD, H₃PO₄) δ 4.8 (s). ¹⁹F NMR (282 MHz, CDCl₃/CD₃OD, CFCl₃) δ -79.5 (s). UV-vis (CHCl₃) λ_{max} (ε) [nm (cm⁻¹ M⁻¹)] 429 (813 000), 557 (48 000), 608 (27 000).

[Pt(dppp)(trans-ZnDPP)]₄[OTf]₈ (15). A solution of 7.5 mg (0.011 mmol) of **4** and 10.0 mg (0.011 mmol) of dpppPt(OTf)₂, **8** in 10 mL of a 3:1 mixture of CHCl₃ and CH₃OH was stirred at room temperature for 5 days. The solvent was reduced in volume, followed by addition of diethyl ether. The brown solid was collected, washed with ether, and dried in vacuo. Yield: 14.4 mg (82%). Mp 310–315 °C dec. ¹H NMR (300 MHz, CDCl₃/CD₃OD) δ 9.41 (br, s, 8H, outer pyrrol H_β), 9.33 (s, 16H, py H_α), 8.76–8.64 (m, 8H, outer pyrrol H_β), 8.25 (m, 16H, inner pyrrol H_β), 8.02–7.86 (m, 28H, porph outer Ph H_{o,p}, py H_β), 7.66–7.38 (m, 88H, porph outer Ph H_m, PhP H_{o,m,p}), 6.90 (br, s, 8H, porph inner Ph H_o), 5.95 (br, s, 12H, porph inner Ph H_{m,p}), 3.58 (16H, PhP-CH₂), 2.43 (m, 8H, PhP-CH₂CH₂). ¹³C{¹H} NMR (125 MHz, CDCl₃/CD₃OD) δ 154.3 (s), 149.4 (s), 141.9 (s), 134.7 (m), 133.8 (m), 132.9 (s), 132.5 (s), 130.1 (s), 127.3 (m), 121.3 (q, *J* = 320 Hz, CF₃SO₃), 114.5 (s), 99.7 (s), 29.9 (s), 18.4 (s). ³¹P{¹H} NMR (121 MHz, CDCl₃/CD₃OD, H₃PO₄) δ -7.8 (*J*_{pt-p} = 3043 Hz). ¹⁹F NMR (282 MHz, CDCl₃/CD₃OD, CFCl₃) δ -74.5 (s). UV-vis (CHCl₃) λ_{max} (ε) [nm (cm⁻¹ M⁻¹)] 433 (1 040 000), 560 (58 000), 608 (39 000).

[Pd(dppp)(trans-DPyTTP)]₄[OTf]₈ (16). To a solution of 15.0 mg (0.017 mmol) of porphyrin **5** in 10 mL of CH₂Cl₂ was added 14.0 mg (0.017 mmol) of dpppPd(OTf)₂, **7**, and the resulting solution was stirred at room temperature for 1 h. The solvent was reduced in volume to 1 mL in vacuo and pentane was added resulting in the formation of a dark-red solid, which was collected, washed with pentane, and dried in vacuo. Yield 28.0 mg (96%). Mp 248–250 °C dec. ¹H NMR (300 MHz, CD₂Cl₂, TMS) δ 10.29 (s, 4H, porph H-20), 9.77 (s, 4H, porph H-10), 9.55 (d, *J* = 5.1 Hz, 16H, py H_α), 8.15–8.10 (m, 48H, py H_β, PhP H_o), 7.75–7.64 (m, 48H, PhP H_o+H_p), 3.99 (m, 16H, outer hexyl (CH₂)(CH₂)₄CH₃), 3.27 (m, 16H, PhP-CH₂), 2.86 (m, 16H, inner hexyl (CH₂)(CH₂)₄CH₃), 2.51 (m, 8H, PhP-CH₂CH₂), 2.22 (m, 16H, outer hexyl CH₂(CH₂)(CH₂)₃CH₃), 2.06 (m, 48H, porph-CH₃), 1.80 (m, 16H, outer hexyl (CH₂)₂(CH₂)(CH₂)₂CH₃), 1.58 (m, 16H, outer hexyl (CH₂)₃-(CH₂)CH₂CH₃), 1.45 (m, 16H, outer hexyl (CH₂)₄CH₂CH₃), 1.15 (m, 16H, inner hexyl CH₂(CH₂)(CH₂)₃CH₃), 0.97 (m, 24H, outer hexyl CH₃), 0.12 (m, 16H, inner hexyl (CH₂)₂(CH₂)(CH₂)₂CH₃), -0.08 (m, 16H, inner hexyl (CH₂)₃(CH₂)CH₂CH₃), -0.25 (m, 16H, inner hexyl (CH₂)₄CH₂CH₃), -0.51 (m, 24H, inner hexyl CH₃), -2.38 (s, 18H, NH). ¹³C{¹H} NMR (75 MHz, CD₂Cl₂, TMS) δ 154.5 (s, py C_γ), 151.1 (s, py C_α), 145.3 (s, porph C₁), 145.2 (s, porph C₆), 144.2 (s, porph C₄, C₆), 142.2 (s, porph C₃, C₇), 135.5 (s, porph C₂), 134.7 (s, porph C₈), 134.2 (s, py C_β), 133.4 (s, PhP C_o), 131.8 (s, PhP C_p), 130.8 (s, PhP C_m), 125.7 (m, PhP C_{ipso}), 119.6 (q, *J* = 319 Hz, CF₃SO₃), 113.0 (s, porph C₅), 98.8 (s, porph C₂₀), 98.4 (s, porph C₁₀), 33.8 (s, outer hexyl CH₂(CH₂)₄CH₃), 32.6 (s, porph outer CH₃), 31.1 (s, inner hexyl CH₂(CH₂)₄CH₃), 30.6 (s, porph inner CH₃), 29.2, 27.2 (all s, outer hexyl), 26.4, 25.1, 24.9, 23.4 (all s, outer and inner hexyls), 22.0 (m, PhP CH₂), 19.0 (s, PhPCH₂CH₂), 17.8, 17.1, 14.5, 13.1 (all s, inner hexyl). ³¹P{¹H} NMR (121 MHz, CD₂Cl₂, H₃PO₄) δ 6.4 (s). ¹⁹F NMR (282 MHz, CD₂Cl₂, CFCl₃) δ -76.1 (s). IR (neat) 2926, 2863, 1608, 1438, 1252, 1155, 1030, 747 cm⁻¹. UV-vis (CH₂Cl₂) λ_{max} (ε) [nm (cm⁻¹ M⁻¹)] 276 (574 000), 414 (634 000), 510 (67 000), 546 (39 000), 580 (36 000), 632 (20 000). Anal. Calcd for C₃₄₈H₄₀₈N₂₄P₈O₂₄S₈F₂₄Pd₄·5H₂O: C, 61.59; H, 6.21; N, 4.96; S, 3.77. Found: C, 61.29; H, 6.11; N, 4.97; S, 3.74. MS (ES) *m/z* 1525.3 (M - 4OTf)⁴⁺ calcd 1525.8.

[Pt(dppp)(trans-DPyTTP)]₄[OTf]₈ (17). A solution of 9.5 mg (0.011 mmol) of porphyrin **5** in 10 mL of CH₂Cl₂ was treated with 10.0 mg (0.011 mmol) of dpppPt(OTf)₂, **8**, and stirred at room temperature for 4 days. The solvent was reduced in volume to 0.5 mL followed by addition of diethyl ether. The brown precipitate was collected, washed with ether, and dried in vacuo. Yield: 16.5 mg (85%). Mp 290–292 °C dec. ¹H NMR (300 MHz, CD₂Cl₂, TMS) δ 10.28 (s, 4H, porph H-20), 9.77 (s, 4H, porph H-10), 9.65 (d, *J* = 4.2 Hz, 16H, py H_α), 8.17–8.12 (m, 48H, py H_β, PhP H_o), 7.75 (t, *J* = 6.9 Hz, 32H,

PhP H_m), 7.67 (t, $J = 7.5$ Hz, 16H, PhP H_p), 3.99 (m, 16H, outer hexyl (CH₂)(CH₂)₄CH₃), 3.33 (m, 16H, PhP-CH₂), 2.84 (m, 16H, inner hexyl (CH₂)(CH₂)₄CH₃), 2.46 (m, 8H, PhP-CH₂CH₂), 2.22 (m, 16H, outer hexyl CH₂(CH₂)(CH₂)₃CH₃), 2.07 (s, 24H, porph outer CH₃), 2.00 (s, 24H, porph inner CH₃), 1.80 (m, 16H, outer hexyl (CH₂)₂(CH₂)(CH₂)₂-CH₃), 1.56 (m, 16H, outer hexyl (CH₂)₃(CH₂)CH₂CH₃), 1.46 (m, 16H, outer hexyl (CH₂)₄CH₂CH₃), 1.13 (m, 16H, inner hexyl CH₂(CH₂)(CH₂)₃-CH₃), 0.97 (m, 24H, outer hexyl CH₃), 0.12 (m, 16H, inner hexyl (CH₂)₂(CH₂)(CH₂)₂CH₃), -0.08 (m, 16H, inner hexyl (CH₂)₃(CH₂)CH₂-CH₃), -0.24 (m, 16H, inner hexyl (CH₂)₄CH₂CH₃), -0.52 (m, 24H, inner hexyl CH₃), -2.36 (s, 8H, NH). ¹³C{¹H} NMR (75 MHz, CD₂Cl₂, TMS) δ 155.2 (s, py C_γ), 151.1 (s, py C_α), 145.6 (s, porph C₁), 145.4 (s, porph C₉), 144.1 (s, porph C₄, C₆), 142.4 (s, porph C₃), 142.2 (s, porph C₇), 135.4 (s, porph C₂), 134.6 (s, porph C₈), 134.3 (s, py C_β), 133.6 (s, PhP C_o), 132.5 (s, PhP C_p), 130.7 (s, PhP C_m), 124.9 (m, PhP C_{ipso}), 121.8 (q, $J = 320$ Hz, CF₃SO₃), 112.7 (s, porph C₅), 99.0 (s, porph C₂₀), 98.5 (s, porph C₁₀), 33.8 (s, outer hexyl CH₂(CH₂)₄CH₃), 32.6 (s, porph outer CH₃), 31.1 (s, inner hexyl CH₂(CH₂)₄CH₃), 30.6 (s, porph inner CH₃), 29.1, 27.2 (all s, outer hexyl), 26.3, 24.7, 23.3, 23.1 (all s, outer + inner hexyls), 21.9 (m, PhP CH₂), 18.9 (s, PhPCH₂CH₂), 17.9, 17.1, 14.5, 13.1 (all s, inner hexyl). ³¹P{¹H} NMR (121 MHz, CD₂Cl₂, H₃PO₄) δ -16.0 (¹⁹⁵Pt satellites, $J_{Pt-P} = 3101$ Hz). ¹⁹F NMR (282 MHz, CD₂Cl₂, CFCl₃) δ -76.5 (s). IR (neat) 2927, 2871, 1610, 1437, 1279, 1254, 1155, 1029, 748 cm⁻¹. UV-vis (CH₂Cl₂) λ_{max} (ϵ) [nm (cm⁻¹ M⁻¹)] 416 (174 000), 512 (17 000), 548 (10 000), 578 (9000), 632 (5000). Anal. Calcd for C₃₄₈H₄₀₈N₂₄P₈O₂₄S₈F₂₄Pt₄·7H₂O: C, 58.22; H, 5.93; N, 4.69; S, 3.57. Found: C, 57.99; H, 5.74; N, 4.62; S, 3.50.

[Pd(dppp)(trans-ZnDPPyTTP)]₄[OTf]₈ (18). To a solution of 4.0 mg (0.0043 mmol) of **6** in 5 mL of CHCl₃ was added 3.5 mg (0.0043 mmol) of dpppPd(OTf)₂, **7**, and the solution was stirred at room temperature for 1 h. The solvent was reduced in volume to 0.5 mL in vacuo. Diethyl ether was then added and the dark-purple precipitate was filtered and dried in vacuo. Yield: 7.4 mg (98%). Mp 224–226 °C dec. ¹H NMR (500 MHz, CD₂Cl₂, TMS) δ 10.26 (s, 4H, porph H-20), 9.69 (s, 4H, porph H-10), 9.54 (d, $J = 5.0$ Hz, 16H, py H_α), 8.17–8.15 (m, 48H, py H_β, PhP H_o), 7.75 (t, $J = 7.3$ Hz, 32H, PhP H_m), 7.69 (t, $J = 7.5$ Hz, 16H, PhP H_p), 3.99 (m, 16H, outer hexyl (CH₂)(CH₂)₄CH₃), 3.25 (m, 16H, PhP-CH₂), 2.74 (m, 16H, inner hexyl (CH₂)(CH₂)₄CH₃), 2.51 (m, 8H, PhP-CH₂CH₂), 2.22 (m, 16H, outer hexyl CH₂(CH₂)(CH₂)₃CH₃), 2.08 (s, 24H, outer porph-CH₃), 1.97 (s, 24H, inner porph-CH₃), 1.81 (m, 16H, outer hexyl (CH₂)₂(CH₂)(CH₂)₂-CH₃), 1.59 (m, 16H, outer hexyl (CH₂)₃(CH₂)CH₂CH₃), 1.47 (m, 16H, outer hexyl (CH₂)₄CH₂CH₃), 1.28 (m, 16H, inner hexyl CH₂(CH₂)(CH₂)₃-CH₃), 0.98 (m, 24H, outer hexyl CH₃), -0.02 (m, 16H, inner hexyl (CH₂)₂(CH₂)(CH₂)₂CH₃), -0.19 (m, 16H, inner hexyl (CH₂)₃(CH₂)CH₂-CH₃), -0.28 (m, 16H, inner hexyl (CH₂)₄CH₂CH₃), -0.55 (m, 24H, inner hexyl CH₃). ¹³C{¹H} NMR (125 MHz, CD₂Cl₂, TMS) δ 156.1 (s, py C_γ), 151.1 (s, py C_α), 147.3 (s, porph C₁, C₉), 146.7 (s, porph C₄, C₆), 145.6 (s, porph C₃), 145.4 (s, porph C₇), 137.2 (s, porph C₂), 136.7 (s, porph C₈), 134.3 (s, py C_β), 133.5 (s, PhP C_o), 132.2 (s, PhP C_p), 130.9 (s, PhP C_m), 125.8 (t, $J = 26.6$ Hz, PhP C_{ipso}), 121.8 (q, $J = 320$ Hz, CF₃SO₃), 114.7 (s, porph C₅), 99.4 (s, porph C₂₀), 99.0 (s, porph C₁₀), 33.8 (s, outer hexyl CH₂(CH₂)₄CH₃), 32.5 (s, porph outer CH₃), 30.9 (s, inner hexyl CH₂(CH₂)₄CH₃), 30.6 (s, porph inner CH₃), 30.3, 29.2 (all s, outer hexyl), 27.2, 26.2, 25.2, 23.4 (all s, outer + inner hexyls), 22.0 (m, PhPCH₂), 19.0 (s, PhPCH₂CH₂), 18.5, 18.2, 14.5, 13.1 (all s, inner hexyl). ³¹P{¹H} NMR (121 MHz, CD₂Cl₂, H₃PO₄) δ 9.0 (s). ¹⁹F NMR (282 MHz, CD₂Cl₂, CFCl₃) δ -74.7 (s). IR (neat) 3107, 2925, 1606, 1436, 1260, 1101, 1029, 801 cm⁻¹. UV-vis (CH₂Cl₂) λ_{max} (ϵ) [nm (cm⁻¹ M⁻¹)] 348 (51 000), 414 (397 000), 542 (35 000), 582 (29 000). Anal. Calcd for C₃₄₈H₄₀₀N₂₄P₈O₂₄S₈F₂₄Pd₄Zn₄·15H₂O: C, 57.89; H, 6.00; N, 4.66; S, 3.55. Found: C, 57.66; H, 5.80; N, 4.83; S, 3.49.

[Pt(dppp)(trans-ZnDPPyTTP)]₄[OTf]₈ (19). A solution of 16.0 mg (0.017 mmol) of **6** and 15.7 mg (0.017 mmol) of dpppPt(OTf)₂, **8**, in 5 mL of CHCl₃ was stirred at room temperature for 5 days. The solvent was reduced in volume, followed by addition of diethyl ether. The brown solid was collected, washed with ether, and dried in vacuo. Yield: 25.4 mg (80%). Mp 260–262 °C dec. ¹H NMR (500 MHz, CD₂Cl₂, TMS) δ 10.22 (s, 4H, porph H-20), 9.98 (s, 4H, porph H-10),

9.70 (d, $J = 5.4$ Hz, 16H, py H_α), 8.18 (m, 48H, py H_β, PhP H_o), 7.78 (t, $J = 7.2$ Hz, 32H, PhP H_m), 7.65 (t, $J = 7.2$ Hz, 16H, PhP H_p), 3.96 (m, 16H, outer hexyl (CH₂)(CH₂)₄CH₃), 3.36 (m, 16H, PhP-CH₂), 2.84 (m, 16H, inner hexyl (CH₂)(CH₂)₄CH₃), 2.50 (m, 8H, PhP-CH₂CH₂), 2.19 (m, 16H, outer hexyl CH₂(CH₂)(CH₂)₃CH₃), 2.06 (s, 24H, outer porph-CH₃), 1.97 (s, 24H, inner porph-CH₃), 1.78 (m, 16H, outer hexyl (CH₂)₂(CH₂)(CH₂)₂CH₃), 1.57 (m, 16H, outer hexyl (CH₂)₃(CH₂)CH₂-CH₃), 1.46 (m, 16H, outer hexyl (CH₂)₄CH₂CH₃), 1.02 (m, 16H, inner hexyl CH₂(CH₂)(CH₂)₃CH₃), 1.00 (m, 24H, outer hexyl CH₃), 0.00 (m, 16H, inner hexyl (CH₂)₂(CH₂)(CH₂)₂CH₃), -0.21 (m, 32H, inner hexyl (CH₂)₃CH₂CH₂CH₃), -0.50 (m, 24H, inner hexyl CH₃). ¹³C{¹H} NMR (125 MHz, CDCl₃, TMS) δ 156.5 (s, py C_γ), 150.7 (s, py C_α), 147.0 (s, porph C₁, C₉), 146.2 (s, porph C₄, C₆), 145.5 (s, porph C₃), 145.0 (s, porph C₇), 136.5 (s, porph C₂), 136.0 (s, porph C₈), 134.0 (s, py C_β), 133.2 (s, PhP C_o), 132.4 (s, PhP C_p), 130.5 (s, PhP C_m), 124.6 (t, $J = 34.9$ Hz, PhP C_{ipso}), 121.4 (q, $J = 318$ Hz, CF₃SO₃), 113.7 (s, porph C₅), 99.3 (s, porph C₂₀), 98.8 (s, porph C₁₀), 33.5 (s, outer hexyl CH₂(CH₂)₄CH₃), 32.2 (s, porph outer CH₃), 32.1 (s, inner hexyl CH₂(CH₂)₄CH₃), 30.6 (s, porph inner CH₃), 30.3, 28.8 (all s, outer hexyl), 27.0, 25.9, 24.8, 23.0 (all s, outer + inner hexyls), 21.6 (m, PhP CH₂), 18.7 (s, PhPCH₂CH₂), 18.3, 18.0, 14.4, 13.0 (all s, inner hexyl). ³¹P{¹H} NMR (121 MHz, CD₂Cl₂, H₃PO₄) δ -14.1 (s, ¹⁹⁵Pt satellites, $J_{Pt-P} = 3086$ Hz). ¹⁹F NMR (282 MHz, CD₂Cl₂, CFCl₃) δ -75.9 (s). IR (neat) 2963, 2927, 2884, 1608, 1439, 1291, 1151, 1031, 699 cm⁻¹. UV-vis (CH₂Cl₂) λ_{max} (ϵ) [nm (cm⁻¹ M⁻¹)] 350 (81 000), 420 (492 000), 546 (48 000), 584 (34 000). Anal. Calcd for C₃₄₈H₄₀₀N₂₄P₈O₂₄S₈F₂₄Pt₄Zn₄·8H₂O: C, 56.11; H, 5.63; N, 4.51; S, 3.44. Found: C, 55.91; H, 5.77; N, 4.44; S, 3.50.

[Pd(dppp)(cis-DPPyDPP)]₂[OTf]₄ (20). To a solution of 10.0 mg (0.012 mmol) of dpppPd(OTf)₂, **7**, in 2 mL of a 3:1 mixture of CHCl₃ and CH₃OH was added 7.5 mg (0.012 mmol) of porphyrin **1** and the resulting solution was stirred at room temperature for 1 h. The solvent was reduced in volume to 1 mL in vacuo and ether was added resulting in the formation of a dark-red solid, which was collected, washed with ether, and dried in vacuo. Yield 16.3 mg (93%). Mp 338–340 °C dec. ¹H NMR (500 MHz, CDCl₃) δ 9.83 (d, $J = 6.0$ Hz, 8H, py H_α), 8.92 (d, $J = 4.5$ Hz, 4H, porph H-2 and H-13), 8.86 (s, 4H, porph H-17 and H-18), 8.58 (s, 4H, porph H-7 and H-8), 8.33 (d, $J = 4.5$ Hz, 4H, porph H-3 and H-12), 8.23–8.17 (m, 16H, py H_β, porph-Ph H_o), 8.07 (m, 16H, PhP H_o), 7.82 (m, 12H, porph-Ph H_m + H_p), 7.66 (m, 16H, PhP H_m), 7.51 (m, 8H, PhP H_p), 3.49 (m, 8H, PhP-CH₂), 2.53 (m, 4H, PhP-CH₂CH₂), -3.00 (s, 4H, NH). ¹³C{¹H} NMR (125 MHz, CDCl₃) δ 153.3 (s, py C_γ), 149.3 (s, py C_α), 141.6 (s, porph C_{17,18}), 134.9 (s, py C_β), 133.7 (s), 132.9 (s), 130.2 (s), 128.4 (s), 127.1 (s), 125.7 (m), 122.7 (s), 121.3 (q, $J = 318$ Hz, CF₃SO₃), 114.7 (s), 29.9 (PhP CH₂), 18.3 (s, PhPCH₂CH₂). ³¹P{¹H} NMR (202 MHz, CDCl₃, H₃PO₄) δ 4.4 (s). ¹⁹F NMR (282 MHz, CDCl₃, CFCl₃) δ -79.4 (s). UV-vis (CHCl₃) λ_{max} (ϵ) [nm (cm⁻¹ M⁻¹)] 268 (72 000), 422 (485 000), 520 (33 000), 556 (17 000), 592 (12 000), 650 (6000). Anal. Calcd for C₁₄₂H₁₀₈N₁₂P₄O₁₂S₄F₁₂Pd₂·5H₂O: C, 57.67; H, 4.02; N, 5.68; S, 4.34. Found: C, 57.51; H, 3.99; N, 5.40; S, 4.37. MS (FAB) m/z 2716.5 (M - OTf)⁺ calcd 2717.4.

[Pt(dppp)(cis-DPPyDPP)]₂[OTf]₄ (21). A solution of 7.3 mg (0.0081 mmol) of dpppPt(OTf)₂, **8**, in 2 mL of a 3:1 mixture of CHCl₃ and CH₃OH was treated with 5.0 mg (0.0081 mmol) of porphyrin **1** and stirred at room temperature for 2 days. The solvent was reduced in volume to 0.5 mL followed by addition of diethyl ether. The brown precipitate was collected, washed with ether, and dried in vacuo. Yield: 9.0 mg (73%). Mp 383–385 °C dec. ¹H NMR (300 MHz, CDCl₃) δ 9.88 (d, $J = 4.2$ Hz, 8H, py H_α), 8.92 (d, $J = 4.8$ Hz, 4H, porph H-2 and H-13), 8.85 (s, 4H, porph H-17 and H-18), 8.57 (s, 4H, porph H-7 and H-8), 8.31 (d, $J = 4.8$ Hz, 4H, porph H-3 and H-12), 8.21 (m, 16H, py H_β, porph-Ph H_o), 8.09 (m, 16H, PhP H_o), 7.82 (m, 12H, porph-Ph H_m + H_p), 7.66 (m, 16H, PhP H_m), 7.49 (m, 8H, PhP H_p), 3.57 (8H, PhP-CH₂), 2.49 (m, 4H, PhP-CH₂CH₂), -2.99 (s, 4H, NH). ¹³C{¹H} NMR (125 MHz, CDCl₃) δ 153.8 (s, py C_γ), 149.4 (s, py C_α), 141.5 (s, porph C_{17,18}), 134.9 (s), 134.7 (s), 133.7 (s), 133.5 (s, py C_β), 133.0 (s), 130.1 (s), 128.4 (s), 127.1 (s), 125.0 (m), 123.0 (s), 121.3 (q, $J = 320$ Hz, CF₃SO₃), 114.4 (s), 29.9 (PhP CH₂), 18.4 (s, PhPCH₂CH₂). ³¹P{¹H} NMR (121 MHz, CDCl₃, H₃PO₄) δ -16.9 (s, ¹⁹⁵Pt satellites, $J_{Pt-P} = 3069$ Hz). ¹⁹F NMR (282 MHz, CDCl₃,

CFCl₃) δ -79.4 (s). UV-vis (CHCl₃) λ_{\max} (ϵ) [nm (cm⁻¹ M⁻¹)] 422 (453 000), 520 (30 000), 556 (15 000), 594 (10 000), 650 (5000). Anal. Calcd for C₁₄₂H₁₀₈N₁₂P₄O₁₂S₄F₁₂Pt₂·6H₂O: C, 54.10; H, 3.84; N, 5.33; S, 4.07. Found: C, 54.03; H, 3.68; N, 5.15; S, 4.03. MS (FAB) *m/z* 2895.8 (M - OTf)⁺ calcd 2895.6.

[Pd(dppp)(cis-ZnDPyDPP)]₂[OTf]₄ (22). A solution of 8.3 mg (0.012 mmol) of **2** in 3 mL of CHCl₃ was added to 10.0 mg (0.012 mmol) of dpppPd(OTf)₂, **7**, in 5 mL of a 3:1 mixture of CHCl₃ and CH₃OH. The resulting solution was stirred at room temperature for 1 h. The solvent was reduced in volume to 0.5 mL in vacuo. Diethyl ether was then added and the dark-purple precipitate was filtered and dried in vacuo. Yield: 17.1 mg (93%). Mp 320–325 °C dec. ¹H NMR (300 MHz, CDCl₃/CD₃OD) δ 9.52 (d, *J* = 4.5 Hz, 8H, py H_a), 8.83 (d, *J* = 4.8 Hz, 4H, porph H-2 and H-13), 8.77 (s, 4H, porph H-17 and H-18), 8.56 (s, 4H, porph H-7 and H-8), 8.22 (d, *J* = 4.8 Hz, 4H, porph H-3 and H-12), 8.11–8.05 (m, 16H, py H _{β} , porph-Ph H_o), 7.94 (m, 16H, PhP H_o), 7.69 (m, 12H, porph-Ph H_m + H_p), 7.55 (m, 16H, PhP H_m), 7.45 (m, 8H, PhP H_p), 3.32 (8H, PhP-CH₂), 2.41 (m, 4H, PhP-CH₂CH₂). ¹³C{¹H} NMR (125 MHz, CDCl₃) δ 154.4 (s), 150.7 (d, *J* = 31 Hz), 148.6 (s), 148.4 (s), 142.9 (s), 134.8 (s), 132.8 (m), 131.0 (d, *J* = 21 Hz), 130.0 (s), 129.3 (s), 127.8 (s), 126.7 (s), 125.3 (m), 123.0 (s), 120.6 (q, *J* = 320 Hz, CF₃SO₃), 115.3 (s), 29.9 (PhP CH₂), 18.1 (s, PhPCH₂CH₂). ³¹P{¹H} NMR (121 MHz, CDCl₃/CD₃OD, H₃PO₄) δ 5.0 (s). ¹⁹F NMR (282 MHz, CDCl₃, CFCl₃) δ -79.3 (s). UV-vis (CHCl₃) λ_{\max} (ϵ) [nm (cm⁻¹ M⁻¹)] 264 (74 000), 318 (51 000), 430 (469 000), 562 (40 000), 604 (18 000). Anal. Calcd for C₁₄₂H₁₀₄N₁₂P₄O₁₂S₄F₁₂Pd₂Zn₂·6H₂O: C, 54.98; H, 3.77; N, 5.42; S, 4.13. Found: C, 54.91; H, 3.77; N, 5.21; S, 3.76.

[Pt(dppp)(cis-ZnDPyDPP)]₂[OTf]₄ (23). A solution of 5.1 mg (0.0075 mmol) of **2** in 1 mL of CHCl₃ was added to 6.8 mg (0.0075 mmol) of dpppPt(OTf)₂, **8**, in 2 mL of a 3:1 mixture of CHCl₃ and CH₃OH. The resulting solution was stirred at room temperature for 1 day. The solvent was reduced in volume to 0.5 mL in vacuo. Diethyl ether was then added and the dark-purple precipitate was filtered and dried in vacuo. Yield: 9.7 mg (82%). Mp 353–355 °C dec. ¹H NMR (500 MHz, CDCl₃/CD₃OD) δ 9.55 (br, s, 8H, py H_a), 8.84 (d, *J* = 4.5 Hz, 4H, porph H-2 and H-13), 8.78 (s, 4H, porph H-17 and H-18), 8.58 (s, 4H, porph H-7 and H-8), 8.21 (d, *J* = 4.5 Hz, 4H, porph H-3 and H-12), 8.10 (m, 16H, py H _{β} , porph-Ph H_o), 7.96 (m, 16H, PhP H_o), 7.68 (m, 12H, porph-Ph H_m + H_p), 7.56 (m, 16H, PhP H_m), 7.45 (m, 8H, PhP H_p), 3.50 (8H, PhP-CH₂), 2.37 (m, 4H, PhP-CH₂CH₂). ¹³C{¹H} NMR (125 MHz, CDCl₃/CD₃OD) δ 155.7 (s, py C _{γ}), 151.0 (s, py C _{α}), 150.3 (s), 148.3 (s), 147.9 (s), 142.7 (s), 134.7 (s), 133.5 (s), 133.0 (m), 132.7 (s), 130.8 (s), 130.0 (s), 127.8 (s), 126.6 (s), 124.8 (m), 123.3 (s), 121.0 (q, *J* = 320 Hz, CF₃SO₃), 114.4 (s), 29.8 (PhP CH₂), 18.2 (s, PhPCH₂CH₂). ³¹P{¹H} NMR (121 MHz, CDCl₃/CD₃OD, H₃PO₄) δ -16.7 (s, ¹⁹⁵Pt satellites, *J*_{Pt-P} = 3025 Hz). ¹⁹F NMR (282 MHz, CDCl₃, CFCl₃) δ -79.4 (s). UV-vis (CHCl₃) λ_{\max} (ϵ) [nm (cm⁻¹ M⁻¹)] 318 (14 000), 434 (186 000), 562 (15 000), 604 (6000). Anal. Calcd for C₁₄₂H₁₀₄N₁₂P₄O₁₂S₄F₁₂Pt₂Zn₂·6H₂O: C, 52.01; H, 3.57; N, 5.13; S, 3.91. Found: C, 51.75; H, 3.67; N, 4.89; S, 3.54.

Cyclotetakis[*cis*-DPyDPP][1,4-bis(*trans*-Pt(PEt₃)₂(OTf))benzene] (24). To a solution of 10.0 mg (0.0081 mmol) of 1,4-bis(*trans*-Pt(PEt₃)₂(OTf))benzene, **11**, in 2 mL of CH₂Cl₂ was added 5.0 mg (0.0081 mmol) compound **1**. The resulting solution was stirred at room temperature for 1 h. The solvent was reduced in volume to 0.5 mL in vacuo. Diethyl ether was then added and the dark-purple precipitate was filtered and dried in vacuo. Yield: 14.3 mg (95%). Mp 220–225 °C dec. ¹H NMR (500 MHz, CD₂Cl₂) δ 9.22 (s, 16H, py H_a), 9.10 (s, 8H, porph H-2 and H-13), 9.04 (s, 8H, porph H-17 and H-18), 8.98 (s, 8H, porph H-7 and H-8), 8.78 (s, 8H, porph H-3 and H-12), 8.64 (s, 16H, py H _{β}), 8.27 (m, 16H, porph-Ph H_o), 7.85 (m, 24H, porph-Ph H_m + H_p), 7.31 (m, 16H, PhP H_o), 1.71 (m, 96H, PCH₂-CH₃), 1.39 (m, 144H, PCH₂CH₃), -2.77 (s, 8H, NH). ¹³C{¹H} NMR (125 MHz, CD₂Cl₂) δ 154.1 (s, py C _{γ}), 151.1 (s, py C _{α}), 141.9 (s), 137.3 (s), 135.2 (s), 133.7 (s), 131.3 (m), 128.8 (s), 127.5 (s), 125.5 (s), 123.4 (s), 121.7 (q, *J* = 319 Hz, CF₃SO₃), 114.9 (s), 13.4 (PCH₂-CH₃), 8.3 (s, PCH₂CH₃). ³¹P{¹H} NMR (121 MHz, CD₂Cl₂, H₃PO₄) δ 17.4 (*J*_{Pt-P} = 2721 Hz). ¹⁹F NMR (282 MHz, CD₂Cl₂, CFCl₃) δ -73.5 (s). UV-vis (CH₂Cl₂) λ_{\max} (ϵ) [nm (cm⁻¹ M⁻¹)] 298 (84 000), 372 (113 000), 424 (1 258 000), 518 (82 000), 556 (48 000), 594

(30 000), 650 (25 000). Anal. Calcd for C₂₉₆H₃₆₈N₂₄P₁₆O₂₄S₈F₂₄Pt₈: C, 47.95; H, 5.00; N, 4.53; S, 3.46. Found: C, 48.02; H, 5.11; N, 4.39; S, 3.26.

Cyclotetakis[*cis*-ZnDPyDPP][1,4-bis(*trans*-Pt(PEt₃)₂(OTf))benzene] (25). To a solution of 10.0 mg (0.0081 mmol) of 1,4-bis(*trans*-Pt(PEt₃)₂(OTf))benzene, **11**, in 2 mL of CH₂Cl₂ was added 5.5 mg (0.0081 mmol) of compound **2**. The resulting solution was stirred at 40 °C for 10 h. The solvent was reduced in volume to 0.5 mL in vacuo. Diethyl ether was then added and the dark-red precipitate was filtered and dried in vacuo. Yield: 13.2 mg (85%). Mp 262–264 °C dec. ¹H NMR (300 MHz, CD₂Cl₂) δ 9.07 (m, 24H, py H_a, porph H-2 and H-13), 8.97 (s, 8H, porph H-17 and H-18), 8.93 (d, *J* = 4.8 Hz, 8H, porph H-7 and H-8), 8.80 (d, *J* = 4.2 Hz, 8H, porph H-3 and H-12), 8.62 (m, 16H, py H _{β}), 8.27 (m, 16H, porph-Ph H_o), 7.81 (m, 24H, porph-Ph H_m + H_p), 7.29 (m, 16H, PhP H_o), 1.70 (m, 96H, PCH₂-CH₃), 1.39 (m, 144H, PCH₂CH₃). ¹³C{¹H} NMR (125 MHz, CD₂Cl₂) δ 156.2 (s), 151.6 (s), 151.0 (s), 150.2 (s), 149.0 (s), 148.7 (s), 143.2 (s), 137.3 (s), 135.1 (s), 133.9 (s), 133.5 (s), 133.2 (s), 131.6 (s), 130.4 (m), 128.1 (s), 127.0 (s), 125.6 (s), 123.7 (s), 120.6 (q, *J* = 319 Hz, CF₃SO₃), 115.1 (s), 13.4 (PCH₂CH₃), 8.3 (s, PCH₂CH₃). ³¹P{¹H} NMR (121 MHz, CD₂Cl₂, H₃PO₄) δ 17.4 (*J*_{Pt-P} = 2732 Hz). ¹⁹F NMR (282 MHz, CD₂Cl₂, CFCl₃) δ -74.3 (s). UV-vis (CH₂Cl₂) λ_{\max} (ϵ) [nm (cm⁻¹ M⁻¹)] 314 (90 000), 432 (1 068 000), 560 (82 000), 602 (31 000). Anal. Calcd for C₂₉₆H₃₆₀N₂₄P₁₆O₂₄S₈F₂₄Pt₈Zn₄·20H₂O: C, 44.28; H, 5.02; N, 4.19; S, 3.19. Found: C, 44.16; H, 4.78; N, 3.89; S, 3.39.

Cyclotetakis[*cis*-Pd(R(+)-BINAP)(OTf)₂](*trans*-DPyDPP) (26). To a solution of 10.0 mg (0.0097 mmol) of Pd(R(+)-BINAP)(OTf)₂, **9**, in 5 mL of CH₂Cl₂ was added 6.0 mg (0.0097 mmol) of *trans*-DPyDPP, **3**. The resulting solution was stirred at room temperature for 20 min and was reduced in volume to 0.5 mL in vacuo. Diethyl ether was then added and the dark brown precipitate was filtered and dried in vacuo. Yield: 14.1 mg (88%). Mp 268–270 °C dec. [α]_D²⁵ +500° (c 3.6 × 10⁻⁵ M, CH₂Cl₂, 20 °C). CD (CH₂Cl₂) λ ($\Delta\epsilon$) [nm (L mol⁻¹ cm⁻¹)] 251 (+416.7), 276 (-20.8), 332 (+166.7), 351 (-104.2), 422 (-975.0), 432 (+833.3). ¹H NMR (300 MHz, CD₂Cl₂) δ 9.34 (s, 8H, py H_a), 9.18 (s, 8H, py H_a), 8.94 (d, *J* = 4.2 Hz, 4H), 8.84 (s, 4H), 8.63 (m, 8H), 8.39–8.16 (m, 40H), 8.10 (s, 4H), 8.02 (d, *J* = 8.4 Hz, 16H), 7.90 (m, 24H), 7.80 (m, 24H), 7.68 (d, *J* = 6.0 Hz, 8H), 7.52 (m, 24H), 7.36 (m, 4H), 7.14 (m, 32H), 6.59 (d, *J* = 8.4 Hz, 16H), 6.18 (m, 8H), -3.24 (s, 4H, NH), -3.33 (s, 4H, NH). ¹³C{¹H} NMR (125 MHz, CD₂Cl₂) δ 154.2 (d, *J* = 27 Hz), 150.5 (m), 142.1 (s), 141.6 (s), 140.7 (m), 137.4 (m), 136.2 (s), 135.5 (s), 135.0 (d, *J* = 28 Hz), 133.8 (s), 133.0 (s), 132.3 (s), 131.8 (m), 131.4 (s), 130.9 (s), 130.0 (s), 129.4 (s), 129.0 (s), 128.1 (m), 127.8 (m), 127.6 (s), 127.2 (s), 126.1 (m), 125.2 (s), 124.7 (s), 121.9 (d, *J* = 34 Hz), 121.7 (q, *J* = 339 Hz, CF₃SO₃), 119.6 (s), 119.1 (s), 115.2 (d, *J* = 49 Hz). ³¹P{¹H} NMR (121 MHz, CD₂Cl₂, H₃PO₄) δ 24.5 (AB, *J* = 18 Hz), 25.0 (AB, *J* = 18 Hz). ¹⁹F NMR (282 MHz, CD₂Cl₂, CFCl₃) δ -77.6 (s). UV-vis (CH₂Cl₂) λ_{\max} (ϵ) [nm (cm⁻¹ M⁻¹)] 290 (246 000), 422 (1 641 000), 518 (100 000), 556 (63 000), 592(31 000), 648 (33 000). Anal. Calcd for C₃₅₂H₂₄₀N₂₄P₈O₂₄S₈F₂₄Pd₄·8H₂O: C, 62.92; H, 3.84; N, 5.00; S, 3.82. Found: C, 62.76; H, 3.93; N, 5.06; S, 3.81.

Cyclotetakis[*cis*-Pd(S(-)-BINAP)(OTf)₂](*trans*-DPyDPP) (27). To a solution of 10.0 mg (0.0097 mmol) of Pd(S(-)-BINAP)(OTf)₂, **10**, in 5 mL of CH₂Cl₂ was added 6.0 mg (0.0097 mmol) of *trans*-DPyDPP, **3**. The resulting solution was stirred at room temperature for 20 min and was reduced in volume to 0.5 mL in vacuo. Diethyl ether was then added and the dark brown precipitate was filtered and dried in vacuo. Yield: 15.1 mg (94%). Mp 268–270 °C dec. [α]_D²⁵ -474° (c 2.8 × 10⁻⁵ M, CH₂Cl₂, 20 °C). CD (CH₂Cl₂) λ ($\Delta\epsilon$) [nm (L mol⁻¹ cm⁻¹)] 251 (-387.5), 276 (+93.8), 332 (-125.0), 351 (+120.8), 422 (+843.8), 432 (-645.8). UV-vis (CH₂Cl₂) λ_{\max} (ϵ) [nm (cm⁻¹ M⁻¹)] 292 (232 000), 422 (1 647 000), 518 (94 000), 554 (57 000), 592 (26 000), 648 (28 000). ¹H, ³¹P, ¹³C, and ¹⁹F NMR spectra of **27** were found to be identical with those of **26**. Anal. Calcd for C₃₅₂H₂₄₀N₂₄P₈O₂₄S₈F₂₄Pd₄·8H₂O: C, 62.92; H, 3.84; N, 5.00; S, 3.82. Found: C, 62.76; H, 3.93; N, 5.06; S, 3.81.

Cyclotetakis[*cis*-Pd(R(+)-BINAP)(OTf)₂](*trans*-ZnDPyDPP) (28). To a solution of 7.6 mg (0.0074 mmol) of Pd(R(+)-BINAP)(OTf)₂, **9**, in 5 mL of CHCl₃ was added 5.0 mg (0.0074 mmol) of *trans*-

ZnDPyDPP, **4**, in a 3:1 mixture of chloroform and methanol. The resulting solution was stirred at room temperature for 40 min and was reduced in volume to 0.5 mL in vacuo. Diethyl ether was then added and the dark brown precipitate was filtered and dried in vacuo. Yield: 10.1 mg (80%). Mp 298–300 °C dec. CD (CH₂Cl₂) λ ($\Delta\epsilon$) [nm (L mol⁻¹ cm⁻¹)], 233 (-300.5), 253 (+333.8), 286 (-115.0), 325 (+89.8), 339 (+23.8), 368 (+84.5). ¹H NMR (300 MHz, CD₂Cl₂) δ 9.34 (s, 8H, py H_a), 9.18 (s, 8H, py H_a), 8.94 (d, *J* = 4.2 Hz, 4H), 8.83 (s, 4H), 8.59 (m, 8H), 8.38–8.16 (m, 40H), 8.09 (s, 4H), 8.02 (d, *J* = 8.4 Hz, 16H), 7.90 (m, 24H), 7.80 (m, 24H), 7.68 (d, *J* = 6.0 Hz, 8H), 7.52 (m, 24H), 7.36 (m, 4H), 7.14 (m, 32H), 6.59 (d, *J* = 8.4 Hz, 16H), 6.17 (m, 8H). ³¹P{¹H} NMR (121 MHz, CD₂Cl₂, H₃PO₄) δ 25.8 (AB, *J* = 18 Hz), 26.2 (AB, *J* = 18 Hz). ¹⁹F NMR (282 MHz, CD₂Cl₂, CFCl₃) δ -77.7 (s). UV-vis (CH₂Cl₂/CH₃OH) λ_{\max} (ϵ) [nm (cm⁻¹ M⁻¹)] 402 (180 000), 424 (1 740 000), 556 (94 000), 555 (34 000).

Cyclobis[*cis*-Pd(*R*(+)-BINAP)(OTf)₂](*cis*-DPyDPP)] (29**).** To a solution of 16.6 mg (0.016 mmol) of Pd(*R*(+)-BINAP)(OTf)₂, **9**, in 10 mL of CH₂Cl₂ was added 10.0 mg (0.016 mmol) of *cis*-DPyDPP, **1**. The resulting solution was stirred at room temperature for 20 min and was reduced in volume to 0.5 mL in vacuo. Diethyl ether was then added and the dark brown precipitate was filtered and dried in vacuo. Yield: 23.5 mg (88%). Mp 278–280 °C dec. [α]_D +1090° (*c* 3.6 × 10⁻⁵ M, CH₂Cl₂, 20 °C). CD (CH₂Cl₂) λ ($\Delta\epsilon$) [nm (L mol⁻¹ cm⁻¹)], 250 (+122.4), 276 (-65.3), 332 (+49.0), 351 (-62.0), 422 (+293.9). ¹H NMR (300 MHz, CD₂Cl₂) δ 9.64 (d, *J* = 4.8 Hz, 4H, py H_a), 9.58 (d, *J* = 4.8 Hz, 4H, py H_a), 8.89 (s, 12H), 8.40 (m, 8H), 8.25–8.07 (m, 20H), 7.99–7.91 (m, 8H), 7.82–7.74 (m, 24H), 7.51 (q, *J* = 7.5 Hz, 12H), 7.32 (s, 4H), 7.13 (q, *J* = 7.8 Hz, 12H), 6.60 (d, *J* = 9.0 Hz, 8H), -2.96 (s, 4H, NH). ¹³C{¹H} NMR (125 MHz, CD₂Cl₂) δ 154.2 (s), 151.1 (s), 150.1 (s), 142.0 (s), 140.8 (s), 136.0 (s), 135.4 (d, *J* = 12 Hz), 135.1 (s), 133.8 (s), 133.4 (s), 132.7 (s), 132.5 (s), 132.3

(s), 130.9 (s), 130.1 (s), 129.3 (s), 129.0 (s), 128.6 (s), 128.3 (s), 127.7 (d, *J* = 11 Hz), 127.4 (s), 125.8 (s), 125.3 (m), 124.7 (s), 122.9 (s), 121.5 (q, *J* = 319 Hz, CF₃SO₃), 119.7 (s), 119.2 (m), 114.9 (s). ³¹P{¹H} NMR (121 MHz, CD₂Cl₂, H₃PO₄) δ 27.3 (s). ¹⁹F NMR (282 MHz, CD₂Cl₂) δ -73.6 (s). UV-vis (CH₂Cl₂) λ_{\max} (ϵ) [nm (cm⁻¹ M⁻¹)], 292 (95 000), 424 (642 000), 520 (39 000), 556 (20 000), 592(13 000), 648 (6000) nm. Anal. Calcd for C₁₇₆H₁₂₀N₁₂P₄O₁₂S₄F₁₂Pd₂·8H₂O: C, 61.59; H, 3.99; N, 4.90; S, 3.74. Found: C, 61.35; H, 3.76; N, 4.57; S, 3.79.

Cyclobis[*cis*-Pd(*S*(-)-BINAP)(OTf)₂](*cis*-DPyDPP)] (30**).** To a solution of 16.6 mg (0.016 mmol) Pd(*S*(-)-BINAP)(OTf)₂, **10**, in 10 mL of CH₂Cl₂ was added 10.0 mg (0.016 mmol) of *cis*-DPyDPP, **1**. The resulting solution was stirred at room temperature for 20 min and was reduced in volume to 0.5 mL in vacuo. Diethyl ether was then added and the dark brown precipitate was filtered and dried in vacuo. Yield: 24.9 mg (94%). Mp 278–280 °C dec. [α]_D -1160° (*c* 5.4 × 10⁻⁵ M, CH₂Cl₂, 20 °C). CD (CH₂Cl₂) λ ($\Delta\epsilon$) [nm (L mol⁻¹ cm⁻¹)], 250 (-81.6), 276 (+63.7), 332 (-40.8), 351 (+57.1), 422 (-302.0). UV-vis (CH₂Cl₂) λ_{\max} (ϵ) [nm (cm⁻¹ M⁻¹)], 288 (100 000), 424 (638 000), 518 (42 000), 554 (21 000), 590(15 000), 646 (7000). ¹H, ³¹P, ¹³C, and ¹⁹F NMR spectra of **30** were found to be identical with those of **29**. Anal. Calcd for C₁₇₆H₁₂₀N₁₂P₄O₁₂S₄F₁₂Pd₂·8H₂O: C, 61.59; H, 3.99; N, 4.90; S, 3.74. Found: C, 61.35; H, 3.76; N, 4.57; S, 3.79.

Acknowledgment. Dedicated to Professor Allen J. Bard on the occasion of his 65th birthday. We thank the National Science Foundation (CHE-9529093) and the National Institute of Health (5R01GM57052) for financial support.

JA9839825